

Ataxia-telangiectasia mutated interacts with Parkin and induces mitophagy independent of kinase activity. Evidence from mantle cell lymphoma

Aloke Sarkar,¹ Christine M. Stellrecht,^{1,2} Hima V. Vangapandu,¹ Mary Ayres,¹ Benny A. Kaiparettu,³ Jun Hyoung Park,³ Kumudha Balakrishnan,^{1,4} Jared K. Burks,⁵ Tej K. Pandita,⁶ Walter N. Hittelman,¹ Sattva S. Neelapu⁴ and Varsha Gandhi^{1,2,5}

¹Department of Experimental Therapeutics, The University of Texas MD Anderson Cancer Center; ²The University of Texas Graduate School of Biomedical Sciences at Houston; ³Department of Molecular and Human Genetics, Dan L. Duncan Comprehensive Cancer Center, Baylor College of Medicine; ⁴Department of Lymphoma/Myeloma, The University of Texas MD Anderson Cancer Center; ⁵Department of Leukemia, The University of Texas MD Anderson Cancer Center and ⁶Department of Radiation Oncology, The Houston Methodist Research Institute, Houston, TX, USA

©2021 Ferrata Storti Foundation. This is an open-access paper. doi:10.3324/haematol.2019.234385

Received: August 9, 2019.

Accepted: January 31, 2020.

Pre-published: February 6, 2020.

Correspondence: *VARSHA GANDHI* - vgandhi@mdanderson.org

Online Supplementary Data

Methods

Cell lines and culture

Cell lines were obtained from either gift or commercial sources MCL cell line Granta-519 was maintained in Dulbecco modified Eagle medium (DMEM, Cellgro) supplemented with 20% FBS while both Jeko-1 and Mino cell lines were maintained in RPMI 1640 medium (ATCC) supplemented with 10% or 20% FBS respectively (A kind gift from Dr Hesham M. Amin, MD Anderson Cancer Center, TX). HEK293, HeLa and A-T fibroblasts (A-T GM16666; and WT GM16667) were obtained from Coriell Cell Repositories and maintained through passage 10 in DMEM (Cellgro) supplemented with 10% FBS. All media were supplemented with 1% penicillin-streptomycin (Invitrogen Inc.). All cell lines were routinely tested for *Mycoplasma* using a MycoTect kit (Invitrogen). MCL, HEK293T (ATCC) and HeLa cell lines were validated by AmpF/STR identification kit (Applied Biosystems) in the MD Anderson cell line validation core facility. Routine cell number and the mean cell volume were determined by Coulter channelyzer (Coulter Electronics, Hialeah, FL).

Patients and primary cell culture

All primary B-cell lymphomas were obtained following informed consent from every patient before inclusion in the study and were in accordance to the declaration of Helsinki. All protocols were approved by the Institutional Review Board at MD Anderson Cancer Center. Malignant lymphocytes from peripheral blood or from apheresis samples were isolated by Ficoll-Hypaque as described (1). Cells were incubated overnight in RPMI 1640 medium (ATCC) supplemented with 20% FBS and 1% penicillin-streptomycin.

Mitochondrial mass, membrane potential and ROS measurements

The mitochondrial mass was determined by staining cells with Mito-Tracker Deep Red FM (M22426, Invitrogen) added directly into cell culture medium (100nM final concentration). For determining mitochondrial membrane potential ($\Delta\Psi_m$), cells were co-stained with 50nM tetramethylrhodamine, ethyl ester perchlorate (TMRE; 87917, Sigma-Aldrich) and incubated at 37°C for 30min, washed in PBS (2X) and analyzed by FCS. Total cellular ROS analysis was performed by loading H₂DCFDA (10 μ M) and incubated in PBS for 15min, washed 1X in PBS and resuspended in complete medium (10% DMEM or 20% RPMI) and acquired by FCS. Mitochondria specific ROS (mROS) analysis was performed by using MitoSOX Red Mitochondrial superoxide indicator dye (M36008, Invitrogen). Cell were stained with the dye (5 μ M final

concentration) and incubated for 10min at 37°C. Cells were washed 1X in PBS before acquiring the data in a FCS Calibur.

Flow cytometry

Briefly 1×10^6 cells were stained with Mitotracker deep red, TMRE, Mito-SOX Red, H₂DCFDA (as stated earlier) or with intracellular staining. Cells were washed in PBS and acquired on a FCS Calibur (BD Biosciences) and analyzed using Flow Jo software (TreeStar) as previously described(1). For apoptosis assay, 1×10^6 cells were stained with Annexin V FITC followed by propidium iodide staining and acquired and analyzed as previously described.

Lentiviral transduction, plasmids and transfection

Five different human Mission shATM clones were obtained from Sigma (TRCN0000010299, TRCN0000039948, TRCN0000039951, TRCN0000194861, and TRCN0000038657). Non-Target shRNA control (SHC002V, Sigma) and shATM clones (2 μ g each) along with 5 μ l Mission Lentiviral packaging mix (SHP001, Sigma) were individually transfected to HEK293T cells in 6 well plate using Fugene 6 transfection reagent (E2691, Promega). 2 ml of each viral supernatant were collected at 48 and 72hr post-transfection resulting in high titer, replication incompetent lentiviral particles following the protocol formulated by Sigma Mission. Exponentially grown MCL (Jeko-1, Mino) and HeLa cells were spin-infected (1000rpm for 90min at RT) in presence of 4 μ g/ml polybrene (Hexadimethrine Bromide; H9268, Sigma) with freshly harvested shATM lentiviral particles. 16hr post spin-infection, cells were washed in 2X PBS and supplemented with regular media. 72hr post spin-infection, cells were started selection with 2 μ g/ml puromycin (P8833, Sigma) for 2 weeks and selected clones were further expanded and analyzed by immunoblot analysis for ATM protein expression.

pcDNA3.1 (+) Flag-His-ATM wt (#31985) and pcDNA3.1 (+) Flag-His-ATM kd (#31986) were obtained from Addgene. GFP-Parkin plasmid was a kind gift from Dr Noriyuki Matsuda, Tokyo Metropolitan Institute of Medical Science, Japan. Both GFP-LC3 and GFP vector plasmids were a kind gift from Dr Min Chen, Baylor College of Medicine, Houston, TX USA. HEK293T, HeLa and A-T cells were transfected with Lipofectamine 2000 (Invitrogen) or Fugene6 (Promega) with the indicated plasmids.

Immunoprecipitation and Co-IP.

Sub-confluent HEK293T, WT-HeLa or A-T cells in 100-mm plates were transiently transfected with 3 μ g of GFP-Parkin, FLAG-ATM (WT or Kd) alone or in combination. 48-72h post-transfection,

cells were lysed in IP-lysis buffer (87787; Pierce) supplemented with protease inhibitors (Roche). Unless otherwise specified, for all IP/co-IP experiments, 5U Benzonase Endonuclease (EM70664-3; Millipore) was added and incubated in RT for 1hr. 5-10% of cell extracts was saved for input control while equal amounts of lysates (500-1000µg) were immunoprecipitated overnight either with mouse anti-ATM (Santa Cruz; sc-23921), rabbit anti-ATM (Millipore; 07-1286), rabbit anti-GFP antibody (Santa Cruz;sc-8334), or mouse anti-Parkin (Santa Cruz; sc-136989) wherever applicable. IP complexes were captured by using Protein A/G-Agarose beads (Santa Cruz; sc-2003) at RT for 1hr. Beads were washed 3 times with lysis buffer and subjected to Immunoblot analysis. For Flag-His-ATM (WT or KD) IP experiments, equal amounts of cell extracts were immunoprecipitated with 25µl/mg protein concentration of EZview anti-Flag M2 Agarose affinity gel (F2426; Sigma) overnight at 4^oc and processed for immunoblot analysis as above. For endogenous co-IP experiments, MCL cell lines (control or treated Jeko-1 and Mino, 30X10⁶ total live cells in each condition) were processed as above.

Measurement of Intracellular Nucleoside Triphosphates by HPLC.

Untreated MCL cell lines (Granta-519, Jeko-1 and Mino), control shRNA and shATM isogenic clones from Jeko-1 and Mino cells (10X10⁶) from three different passages were collected and cell pellets were stored in -80°C until use. Similarly three separate passages from A-T isogenic cells were collected (5X10⁶) and stored identically until processing. Intracellular nucleotides were extracted using perchloric acid and the extracts were neutralized with KOH as previously reported(2). All neutralized extracts were passed through an anion-exchange Partisil-10 SAX column and eluted at a flow rate of 1.5 ml/min with a 50-min concave gradient (curve 7; Waters 600E System Controller; Waters Corp.) from 60% 0.005 M NH₄H₂PO₄ (pH 2.8) and 40% 0.75 M NH₄H₂PO₄ (pH 3.6) to 100% 0.75 M NH₄H₂PO₄ (pH 3.6). The column elute was monitored by UV absorption at 256 nm, and the nucleoside triphosphates were quantitated by electronic integration with reference to external standards. The intracellular concentration of nucleotides in the extract was then calculated from the mean volume and number of cells used. Cell number was used routinely by using a Coulter counter (Coulter Electronics, Hialeah, FL).

Oxygen consumption analyses

Stable control shRNA and shATM clones from Jeko-1 and Mino cells were analyzed for oxygen consumption rate (OCR) following puromycin selection. 48hr before assay, the cells were resuspended in antibiotic free media. 8×10⁴ cells were plated onto Cell-Tak coated XF96 microplates (Seahorse Bioscience, Massachusetts, USA). Regular RPMI 1640 was replaced with

175µL XF base medium supplemented with 10mM Glucose and 2mM Sodium Pyruvate. Each cell line in an individual experiment had 5 technical replicates and was repeated n=4. Respiration was measured sequentially after addition of Oligomycin (1.25µM), FCCP (1µM), Antimycin A and Rotenone (1µM) were injected in the order listed for XF cell mitochondrial stress test (3). Similarly, WT and A-T cells (10⁴ cells were plated for analysis) were assayed for OCR.

Cell Fractionation

MCL and HeLa cells (30 or 10X10⁶ per treatment) were subjected to whole cell, nuclear, cytoplasmic, and mitochondrial fractionation. Nuclear and cytoplasmic fractionations were made by using NE-PER kit (Thermo Fisher) according to manufacturer's instruction. Purified mitochondrial fraction was prepared by using a Cell fractionation kit (Abcam; AB109719) following manufacturer's guidelines. For trypsin digestion, isolated mitochondria were suspended in buffer M (10 mM HEPES-KOH pH7.4, 250 mM sucrose, 0.5 mM EGTA, 2 mM EDTA, 1 mM DTT). Trypsin was added to final concentration 10 mg/ml and left at room temperature for 30min and terminated by adding equivalent amount of trypsin inhibitor, followed by washing in buffer M for 5 times. Following this, trypsin-digested mitochondrial protein was isolated by Buffer C according to manufacturer's guidelines. All kit components (except Buffer M) were supplemented with protease inhibitor cocktail (cOmplete, Protease and PhosSTOP inhibitors; Sigma-Aldrich) before use.

Western blot analysis

Total protein extracts were prepared by lysing cells in RIPA lysis buffer (Thermo Fisher; 89900) supplemented with protease inhibitor. Protein extracts (10-50 µg) were run on a Criterion precast 4-12% gradient gel (Bio Rad), transferred onto a PVDF membrane (Bio Rad) for overnight at 4°C. Blots were cut into pieces and blocked with either Odyssey blocking buffer (LI-COR Inc), or 5% milk (for ECL exposure) for 2hr and probed with primary antibodies overnight at 4°C, followed by 3X washes with TBS-Tween-20. Membranes strips were incubated with infrared-labeled appropriate secondary antibodies (LI-COR Inc) for 1 hr, scanned, and visualized using LI-COR Odyssey Infrared Imager. For ECL blots, appropriate peroxidase-coupled secondary antibodies were incubated for 1hr at room temperature followed by 3X washes and exposed to premium X-ray film (Phenix).

B cell isolation, IR treatment, phospho-γH2AX and phospho-ATM Intracellular staining

B cells were isolated from healthy donor by using EasySep Human Negative B Cell Enrichment Kit (19054; Stem cell Technologies) according to manufacturer's guideline. Primary apheresis lymphomas were purified by Ficoll-Hypaque differential centrifugation. Purified primary cells, B cells from healthy donors or MCL cell lines were subjected to IR (5-25X10⁶ total cells, 5 Gray in total, 0.3 Gray/min). Alternatively, cells were also treated with *Neocarzinostatin* (NCS, 40nM for 1hr) to induce DNA damage. Following IR-induced DNA damage, cells were kept at 37°C for 30min-1hr and fixed in standard cold 70% ethanol. Cells were permeabilized with intracellular staining PARM wash buffer (421002; BioLegend), followed by 1X wash in the same buffer. Cells (1X10⁶ total) were incubated with FITC anti-H2A.X Phospho^{Ser139} (613403; BioLegend) and PE anti-ATM Phospho^{Ser1981} (613403; BioLegend) in cell staining buffer (42020; BioLegend) for 1hr at room temperature according to manufacturer's guideline. Cells were washed 2X with PARM wash buffer and stained cells were acquired by flow cytometer.

Total RNA extraction and quantitative real-time reverse transcription-PCR

Total RNA from MEF cells was extracted using RNeasy Mini Kit (Qiagen, 74106), and quantitated using NanoDrop ND 1000 spectrophotometer (Thermo Fisher Scientific). Reverse transcription reaction from 100 ng total RNA template was performed using RevertAidTM H Minus First Strand cDNA Synthesis Kit using random primers (Thermo Fisher Scientific) according to the manufacturer's guidelines. The following gene specific primers were designed with NCBI-Primer Designing Tools: ATM (5'-FTGCACTGAAAGAGGATCGTAAA-3'; R: 5'-CAGAGGGAACAAAGTCGGAATA-3'), GFP (F: 5'-AGTCCGCCCTGAGCAAAGA-3'; R: 5'-TCCAGCAGGACCATGTGATC-3'), and 18s (F: 5'-GGCCCTGTAATTGGAATGAGTC-3'; R: 5'-CCAAGATCCAACACTACGAGCTT-3') obtained from Sigma GenoSys, Woodlands, TX. Real-time PCR was performed by using the SYBR® Green PCR Master Mix (Thermo Fisher Scientific) with forward and reverse primers at a final concentration of 10 µM and added according the manufacturer's instructions (Thermo Fisher Scientific). Each cDNA sample was assayed in triplicate, in a 7900HT fast real-time PCR system (Applied Biosystems) with the following cycling conditions: 10 min at 95°C (1 cycle); 15s at 95°C; and 1 min at 60°C (total 40 cycles). The expression was normalized to 18s RNA, and the results are presented as levels relative to the levels in the ATM WT cells (4).

Confocal analysis

Exponentially growing HeLa cells (5X10³) from control or shATM clones were grown overnight in 2 well Nunc Lab-Tek chamber slides (154461, Thermo Fisher). One well from each chamber was

treated with CCCP and the other well was treated with DMSO (0.01% for 3hr). Following 2X wash with 1XPBS, cells were fixed in standard 2% paraformaldehyde, permeabilized with 0.2% Triton X-100(5), blocked in 5% normal horse serum (S-2000; Vector Lab) supplemented with 2% BSA (A8531; Sigma-Aldrich) and stained with rabbit anti-ATM (Millipore; 1:200), mouse anti-Tom20 (Santa Cruz; 1:150) or with mouse anti-DNA (AC-30-10; Progen; 0.01 μ g) overnight at 4°C followed by 3X washes in 1X PBS (5 min each). The slides were incubated with Donkey anti-Rabbit Alexa Fluor 488 (A-21206; Thermo Fisher Scientific; 1:500) and Goat anti-Mouse Alexa Fluor 555 (A-2422; Thermo Fisher Scientific; 1:500) for 1hr at room temperature, followed by 3X Washes for 5min each in 1XPBS. After immunolabeling, slides were mounted in SlowFade® Gold Antifade Mountant with DAPI (Life Technologies; S36938).

Images were captured using an Olympus FV1000 laser confocal microscope with a 40x 1.3 oil immersion lens. Images were loaded into 3i's Slidebook 5.5 software for analysis. Using the DAPI staining, a mask of the nucleus was determined. The other fluorescent channels, including the auto-fluorescent noise, were used to determine a whole cell mask. The nuclear mask was subtracted from the whole cell mask to identify the cytoplasmic space. Focal expression was identified using a Laplace filter of the ATM and Tom20 channels (green and red channels). Depending on the desired metric, channels were either compared to determine if expression existed in the same pixel or voxel or a cross mask was used to determine the number of foci present in the nuclei, mitochondria, or cytoplasmic spaces. These were then plotted and mean numbers were determined for comparison across various conditions. All captured data were analyzed using 3i's Slidebook 5.5 (SB645.0.0.30) software.

References

1. Balakrishnan K, Nimmanapalli R, Ravandi F, et al. Forodesine, an inhibitor of purine nucleoside phosphorylase, induces apoptosis in chronic lymphocytic leukemia cells. *Blood*. 2006;108(7):2392-2398.
2. Gandhi V, Ayres M, Halgren RG, et al. 8-chloro-cAMP and 8-chloro-adenosine act by the same mechanism in multiple myeloma cells. *Cancer Res*. 2001;61(14):5474-5479.
3. Ferrick DA, Neilson A, Beeson C. Advances in measuring cellular bioenergetics using extracellular flux. *Drug Discov Today*. 2008;13(5-6):268-274.
4. Livak KJ, Schmittgen TD. Analysis of relative gene expression data using real-time quantitative PCR and the 2(-Delta Delta C(T)) Method. *Methods*. 2001;25(4):402-408.
5. Sarkar A, Balakrishnan K, Chen J, et al. Molecular evidence of Zn chelation of the procaspase activating compound B-PAC-1 in B cell lymphoma. *Oncotarget*. 2016;7(3):3461-3476.

Supplementary data Figure Legends

Figure S1. ATM dependent mitophagy in A-T isogenic cells.

(A). Annexin V-PI apoptosis assay in MCL cell lines treated with FCCP (75 μ M for 4hr) showing representative FCS analysis and relative live cell fractions were plotted (n=3; Mean \pm SEM; *p<0.05 significant difference from DMSO control).

(B). Representative FCS profile of A-T isogenic cell lines (2X10⁶ cells) treated with CCCP (75 μ M for 3hr) and stained with TMRE (PE) or Mitotracker deep red (APC), and acquired by FCS Caliber and analyzed by FlowJo. Relative geomean of mitochondria showing CCCP-induced mitophagy in A-T isogenic cells. (n=5; Mean \pm SEM; **p<0.001 significant difference from respective DMSO control).

(C) Relative geomean of $\Delta\Psi_m$ during CCCP-induced mitophagy in A-T isogenic cells. (n=5; Mean \pm SEM; *p<0.05 significant difference from respective DMSO control).

(D) Immunoblot analysis (50 μ g total protein) followed by densitometry analysis (n=5; showing relative Tom20 expression) from A-T isogenic cells treated with CCCP. Separate blots were cut into pieces and probed with the indicated antibodies. Pink1 and Parkin blots were detected by ECL method. GAPDH was probed for loading control each time.

(E). Representative FCS profile of MitoSOX Red staining showing mROS levels in untreated A-T isogenic cells.

(F) Relative geomean of basal mROS in A-T isogenic cells (n=4; **p<0.001 significant difference from WT cells).

Figure S2: Cell fractionation analyses in MCL cell lines revealed extra-nuclear ATM.

(A) Cell fractionation immunoblot analysis of MCL cell lines (30X10⁶ cells per treatment as shown in main text Figure 1h) showing basal and FCCP (75 μ M for 3hr)-induced mitophagy showing nuclear (10 μ g) and cytoplasmic (10 μ g) fractions probed with indicated antibodies. Lamin and GAPDH were probed to distinguish nuclear and cytoplasmic proteins. Separate sets of blots were probed using Licor or ECL methods of detection (see methods), cut into pieces and probed with the indicated antibodies.

(B). Densitometry analysis showing relative activated Parkin (phospho-UB^{Ser65}) expression following FCCP (75 μ M for 3hr) treatment in whole cell or mitochondrial fractions in MCL cell lines (n=3; Mean \pm SEM; *p<0.05; significant difference from respective DMSO control).

Figure S3. Loss of ATM confers resistance to FCCP-induced mitophagy in MCL cell lines.

(A) Cell fractionation immunoblot analysis of MCL shATM clones showing total and mitochondrial ATM (10 μ g protein loaded in each fractions) treated with control (C: DMSO) or FCCP (F: 75 μ M for 3hr). Blot was cut into pieces and probed with indicated antibodies. GAPDH was probed to distinguish total and mitochondrial fractions.

(B). qPCR analysis of mtDNA copy number in A-T isogenic cells showing mean \pm SEM; n=5; ****p<0.0001 significant difference from A-T cells.

(C). Relative geomean of $\Delta\Psi_m$ in FCCP-treated (as in Figure. 2E) control or shATM MCL clones (n=4; Mean \pm SEM; ****p<0.0001; ***p<0.001; significant difference from respective control shRNA).

Figure S4. Lower ATP and UTP in Granta-519 and intrinsic defect in oxygen consumption in A-T cells.

(A). HPLC analysis of basal and untreated intracellular nucleotide levels in MCL cell lines showing mean \pm SEM (n=3). *p<0.05 significant difference in Jeko-1 UTP, Mino UTP or Mino ATP levels compared to Granta-519.

(B). Graphical representation (as in Figure 3B main text) of Seahorse XF96 analysis of mitochondrial stress test assay (OCR) in A-T isogenic cells (5 \times 10⁴ live cells).

(C). Relative basal OCR in A-T isogenic cells showing mean \pm SEM; (n=5; ***p<0.0001 significant difference from WT cells.

Figure S5. Loss of GFP-Parkin expression in shATM HeLa cells.

(A). WT and Kd HeLa cells treated with DMSO or CCCP (as in Figure 4B-D) were processed for confocal analysis with anti-ATM or anti-Tom20 antibodies and images were captured using an Olympus FV1000 laser confocal microscope for detecting ATM localization into different cellular compartments (see method). Using DAPI, a nuclear mask was generated. The other fluorescent

channels captured including the auto fluorescence were used to determine a whole cell mask. The nuclear mask was then subtracted from the whole cell mask to identify the cytoplasmic space. Using the Tom20 signal, the mitochondrial mask was generated. Images showing respective masks generated for calculation of global ATM distribution (scale: 10 μ m).

(B). WT and Kd HeLa cells were transiently transfected with 3 μ g of GFP-Parkin plasmids. 96hr following transfection, MG132 (10 μ M) or DMSO (as in Figure 5A) were added for 4,8 or 12hr. Single cells were prepared and acquired by FCS Caliber and analyzed by FlowJo for GFP expression. FCS data showing superimposed images with corresponding geomean values of respective GFP expression.

Figure S6. ATM kinase independent ATM-Parkin interaction.

(A). Representative immunoblot analysis IP with of anti-ATM antibody and probed with both GFP (related to Figure 5E) or ATM antibody showing pulldown efficacy in WT HeLa cells. The ratio of the co-IPs were determined by densitometry analysis are shown below indicating little or no effect on their binding affinity following the indicated treatments. Data showing Mean \pm SEM (n=3); no significant difference from respective DMSO control.

(B). Representative Immunoblot analysis of IP of endogenous Mino cell proteins with either anti-Parkin or anti-ATM and probed with both targets to show the pulldown efficacy (related to Figure 5G). The ratio of the co-IPs were calculated and shown (Mean \pm SEM; n=4) indicating little or no effect on their binding affinity following the indicated treatments.

(C) Kd HeLa cells were transiently co-transfected with 3 μ g each GFP-Parkin and WT-Flag-His-ATM or KD-Flag-His-ATM or control pcDNA plasmids. 48hr later cells were immunoprecipitated (500 μ g) with EZview anti-Flag M2 Agarose affinity gel and probed with either rabbit anti-GFP or mouse anti-Parkin antibodies. Arrows indicate specific GFP, Parkin or superimposed bands. 10 μ g pcDNA+GFP-Parkin transfected control extract was loaded to show specificity for GFP-Parkin band. Bottom showing immunoblot analysis of FLAG to show the pulldown efficacy.

(D) Input controls (5%) showing Flag-ATM or GFP-Parkin specific merged bands. Blots were cut into pieces and probed with the indicated antibodies. GAPDH served as loading control.

Figure S7. ATM kinase activity is dispensable in mitophagy in MCL and A-T cell lines

(A) Geomean of mitochondrial $\Delta\Psi_m$ in MCL cell lines treated with FCCP (as in Figure 6A,B). Cells were treated with KU60019 either alone or in combination with FCCP. Following treatments, cells were washed and stained with TMRE (PE) and acquired by FCS Caliber and analyzed by FlowJo. Data showing mean \pm SEM; n=7; ****p<0.0001 significant difference from respective DMSO controls.

(B). Geomean of mitochondrial mass in WT cells treated with CCCP (75 μ M for 3hr) or KU60019 (10 μ M for 1hr) either alone or in combination. Data showing mean \pm SEM; n=3; *p<0.05 significant difference from respective DMSO or KU60019 controls.

(C). Densitometry analysis showing relative activated Parkin (phospho-UB^{Ser65}) in Jeko-1 and Mino cell lines treated with FCCP, KU60019 or both (as in Figure 6A,B). Data (n=3) showing Mean \pm SEM; *p<0.05; significant difference from respective DMSO control).

(D). Densitometry analysis (as above, Figure S7C) showing relative Pink1 activation following identical treatments in Jeko-1 and Mino cells (related to Figure 6A,B). Data (n=4) showing Mean \pm SEM; ***p<0.0001; *p<0.05 significant difference from respective DMSO control).

Figure S8. ATM kinase independent mitophagy in primary B-cell lymphomas.

(A). Representative FCS profile of isolated B-cells from 5 healthy donors (3 purified B-cells and 2 from PBMC). 5X10⁶ live cells were treated with FCCP (75 μ M for 3hr) and stained with TMRE (PE) or Mitotracker deep red (APC) (upper panel). IR-induced (5gr) ATM^{Ser1981} and γ H2AX^{Ser139} phosphorylation (lower panel). Cells were acquired by FCS Caliber and analyzed by FlowJo.

(B) Representative FCS profile of 21 primary MCL subject subjects (Table 1) showing FCCP-Induced (75 μ M for 3hr) mitophagy (upper panel) or IR-induced (5gr; lower panel) ATM^{Ser1981} and γ H2AX^{Ser139} phosphorylation (as in 8A).

(C). Representative FCS profile of 6 primary DLBCL lymphomas.

(D). Representative FCS profile of 6 primary FL lymphomas.

(E). Representative FCS profile of 5 primary MZL or SMZL lymphomas.

Figure S9. Differential FCCP-induced mitophagy in subtypes of B- cell lymphomas

(A). Line graph representation of FCCP-induced mitophagy showing geomean of mitochondrial mass from 4 healthy donors (3 purified B cells and 1 from PBMC) or from 17 primary non-MCL lymphomas (DLBCL=6; FL=6, MZL=5) and their response to IR (Supplementary Table S3).

(B). qPCR (as in Figure 6L) of mtDNA copy number analyses from 17 primary non-MCL lymphomas showing their respective IR status. *** $p < 0.0005$ significant difference in FL lymphomas (Supplementary Table S3). WT DNA and Rho0-DNA served as positive and negative controls respectively.

(C). Relative geomean (Supplementary Table S3) showing mROS levels in untreated B cells isolated from healthy donors (n=3) or from 14 primary non-MCL (FL=5; MZL=4 and DLBCL=5) lymphomas corresponding to their respective IR status.

(D). Line graph representation of FCCP-induced mitophagy showing geomean of $\Delta\Psi_m$ (as in Figure 6N) from 4 healthy donors (3 purified B cells isolated and 1 from PBMC) or from 17 primary non-MCL lymphomas (DLBCL=6; FL=6, MZL=5) and their response to IR (Supplementary Table S3).

Figure S10. Immunoblot analysis of FCCP-induced mitophagy in B- cell lymphomas

(A) Immunoblot analysis showing FCCP-induced mitophagy in control B cells, MCL cell lines or from primary MCL lymphoma samples (10-30 μ g total protein) and probed with indicated antibodies. Corresponding IR or FCCP-induced FCS analysis data are shown in table underneath. Parkin, phospho-UB^{ser65} Parkin and Pink1 protein expressions were detected by ECL method. Both actin and GAPDH were probed for loading controls.

(B) Immunoblot analysis showing FCCP-induced mitophagy in Mino MCL cell line or from primary MCL lymphoma samples (30 μ g total protein) or

(C) Jeko-1 MCL cell line or from primary MCL lymphomas (10-30 μ g total protein) or

(D) Mino MCL cell line or from primary MCL lymphomas (20-30 μ g total protein) or

(E) Jeko-1 MCL cell line or from primary MZL lymphomas (20-30 μ g total protein) or

(F) Mino MCL cell line or from primary DLBCL lymphomas (10-30 μ g total protein) or

(G) Jeko-1 MCL cell line or from primary DLBCL and FL lymphomas (10-30 μ g total protein) or

(H) Mino MCL cell line or from primary FL lymphomas (10-30 μ g total protein).

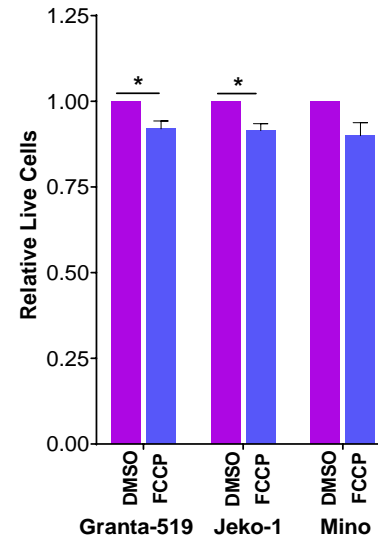
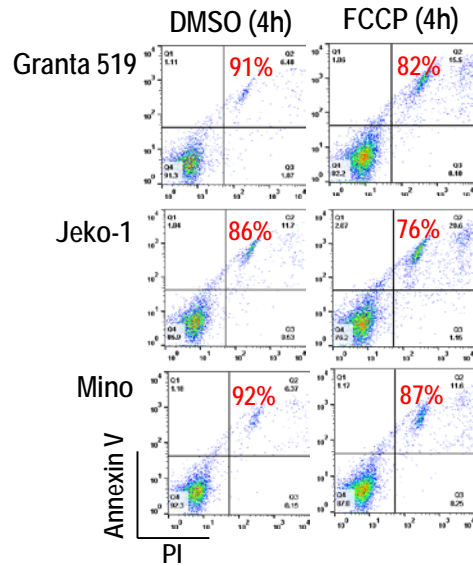
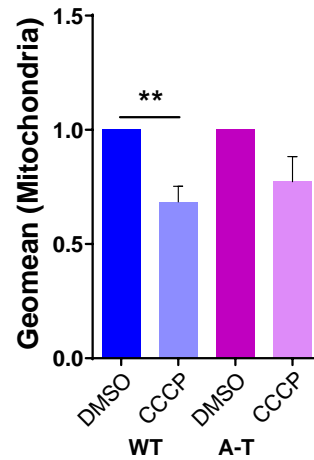
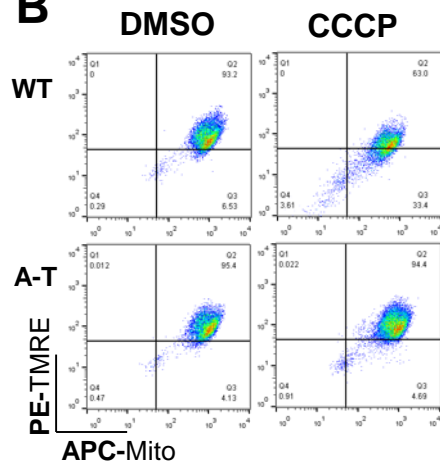
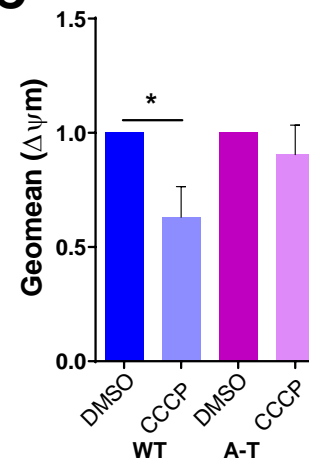
A**B****C**

Figure S1

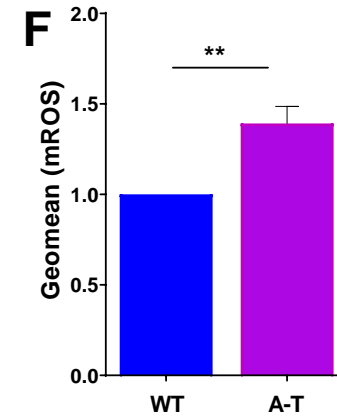
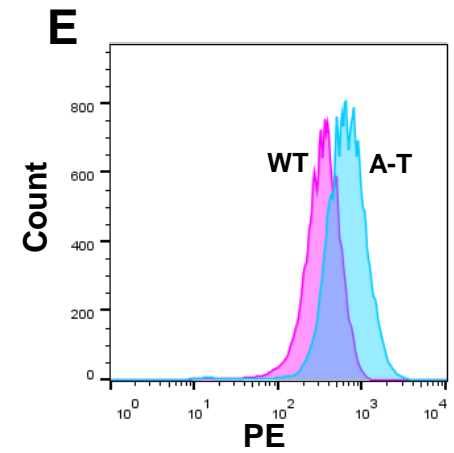
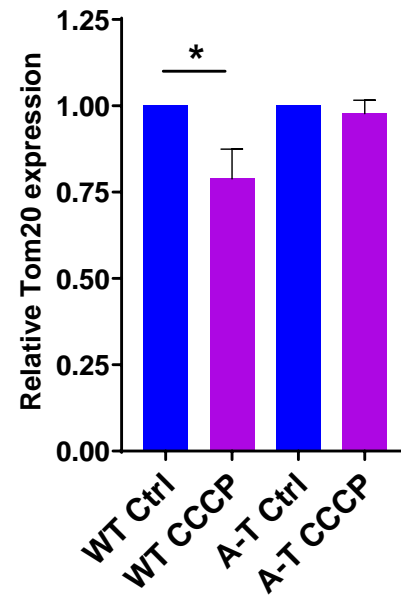
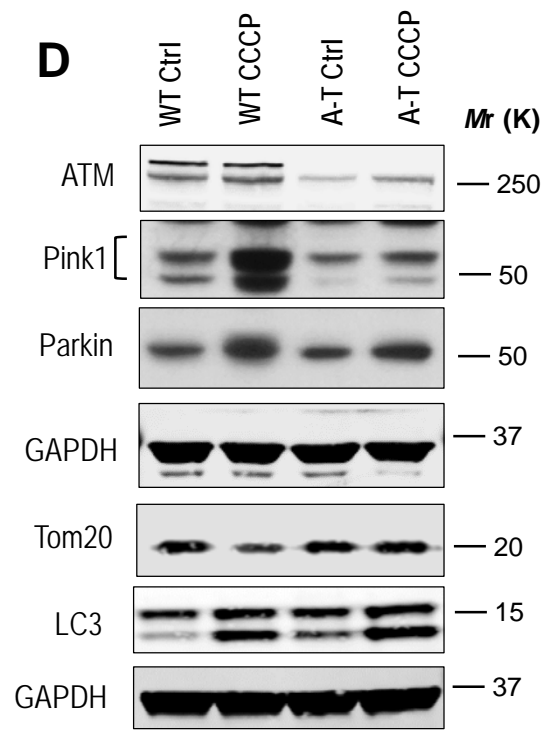


Figure S1

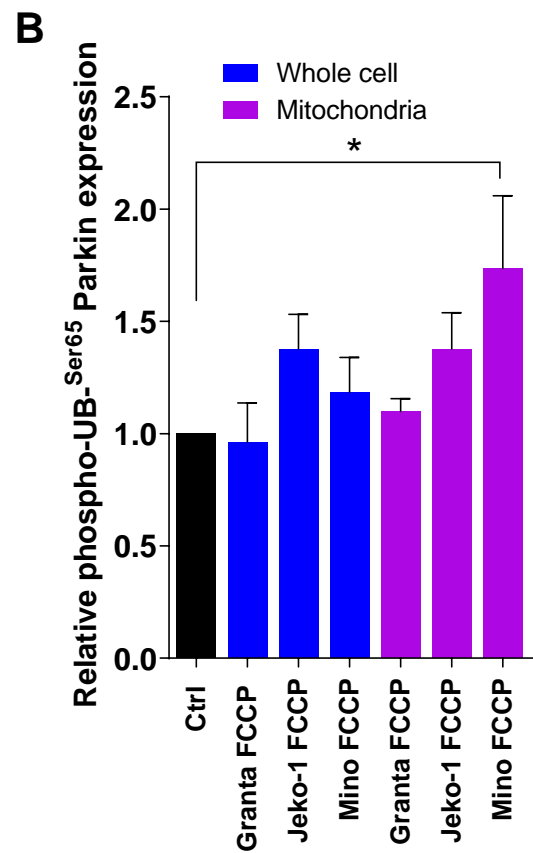
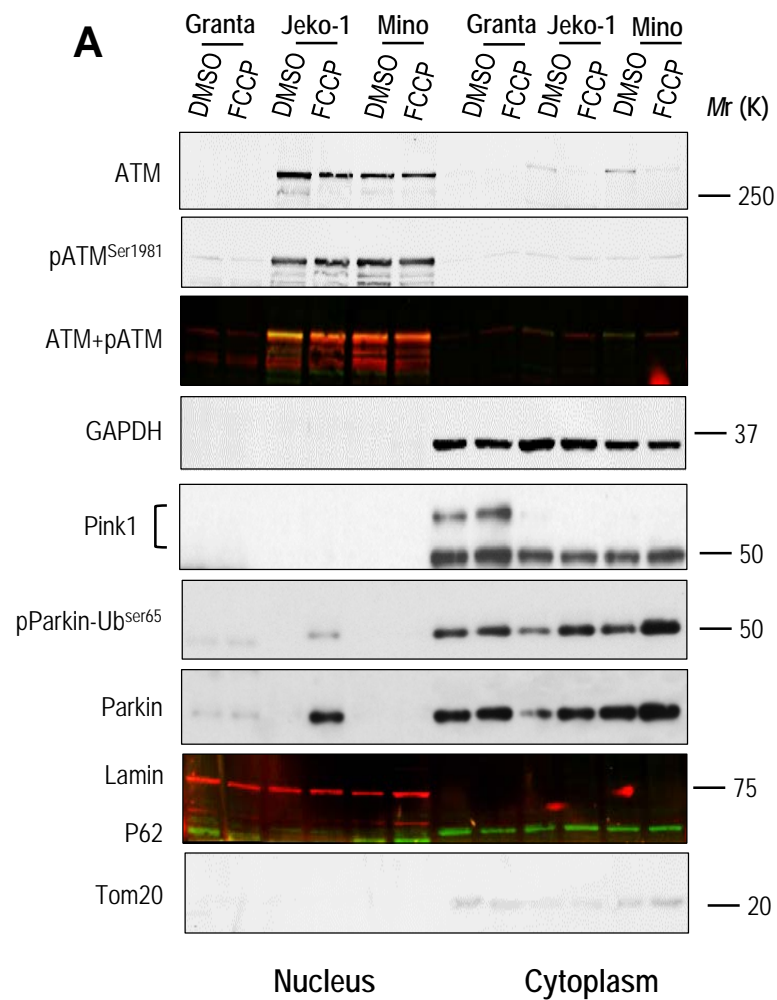


Figure S2

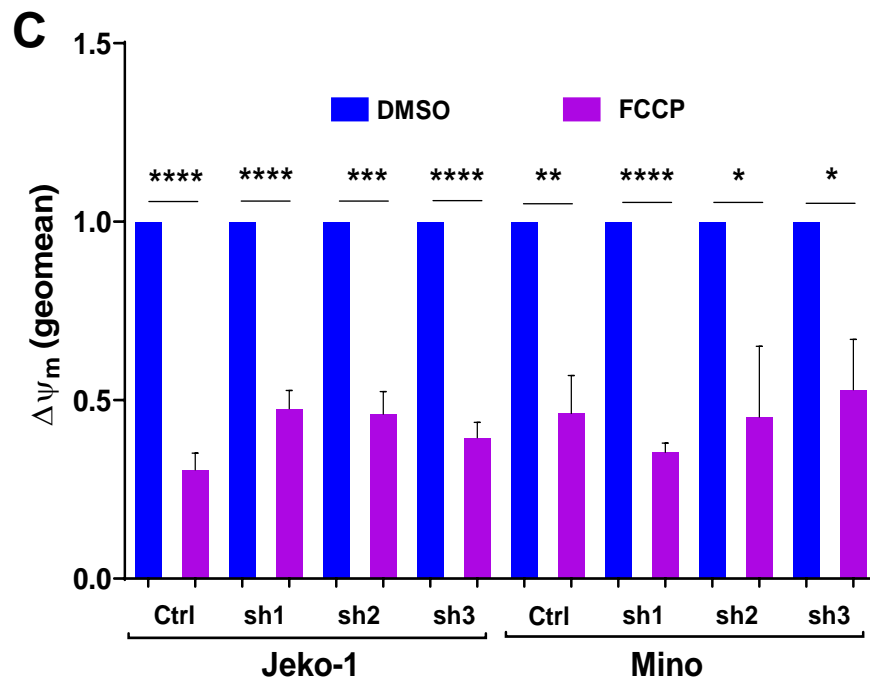
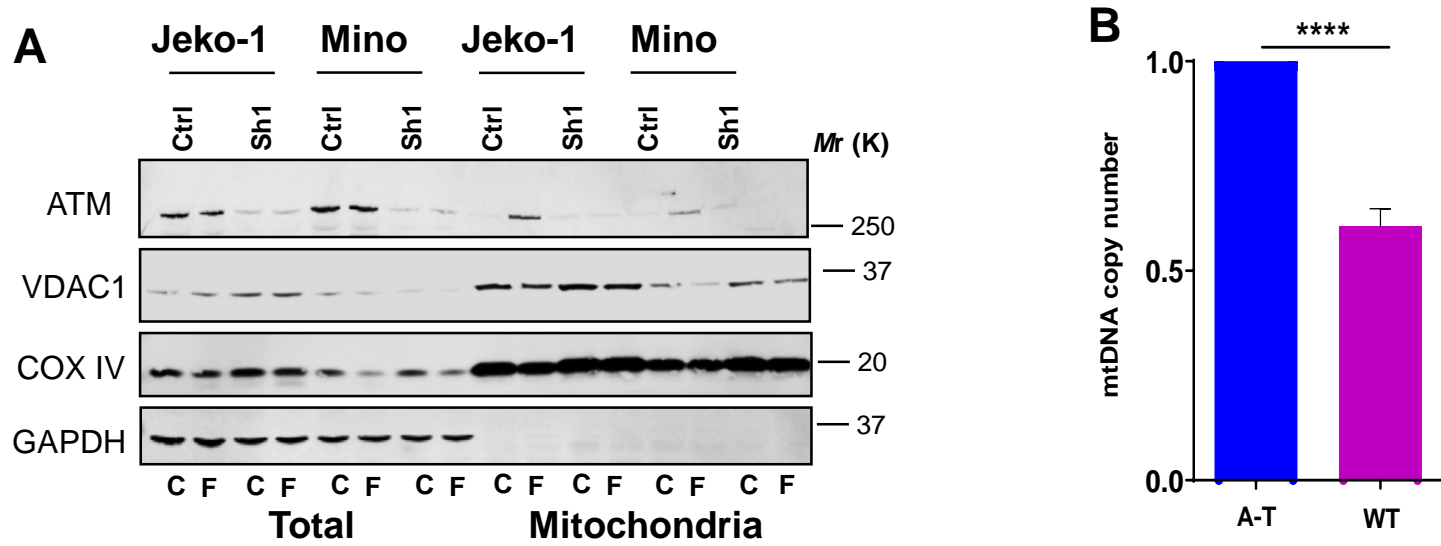


Figure S3

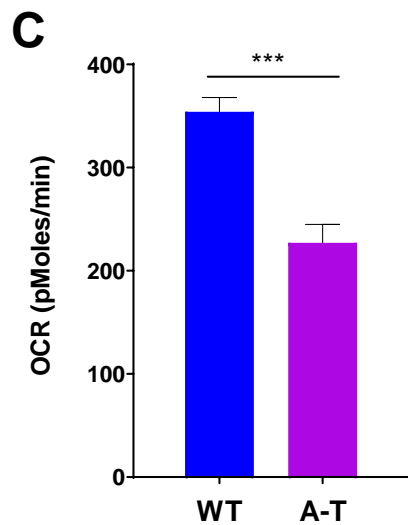
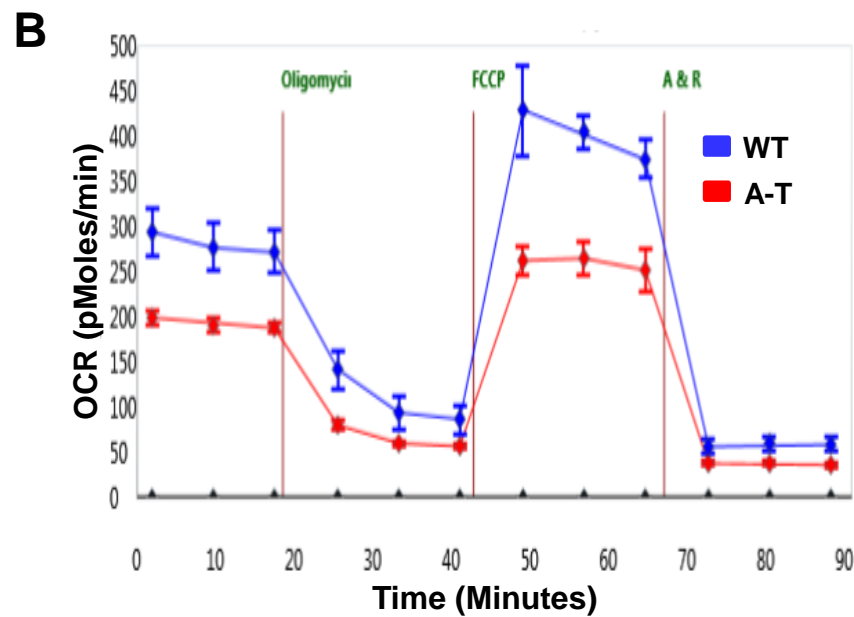
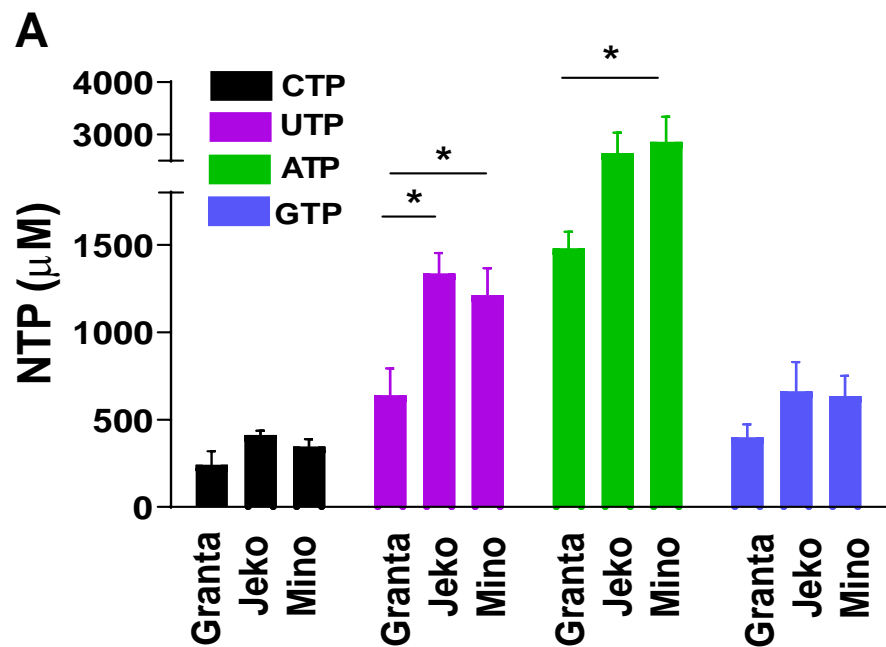


Figure S4

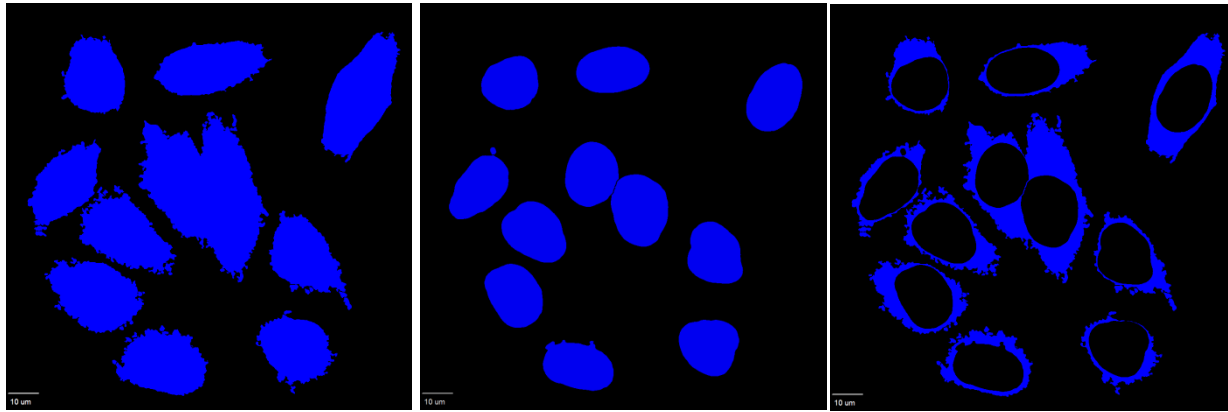
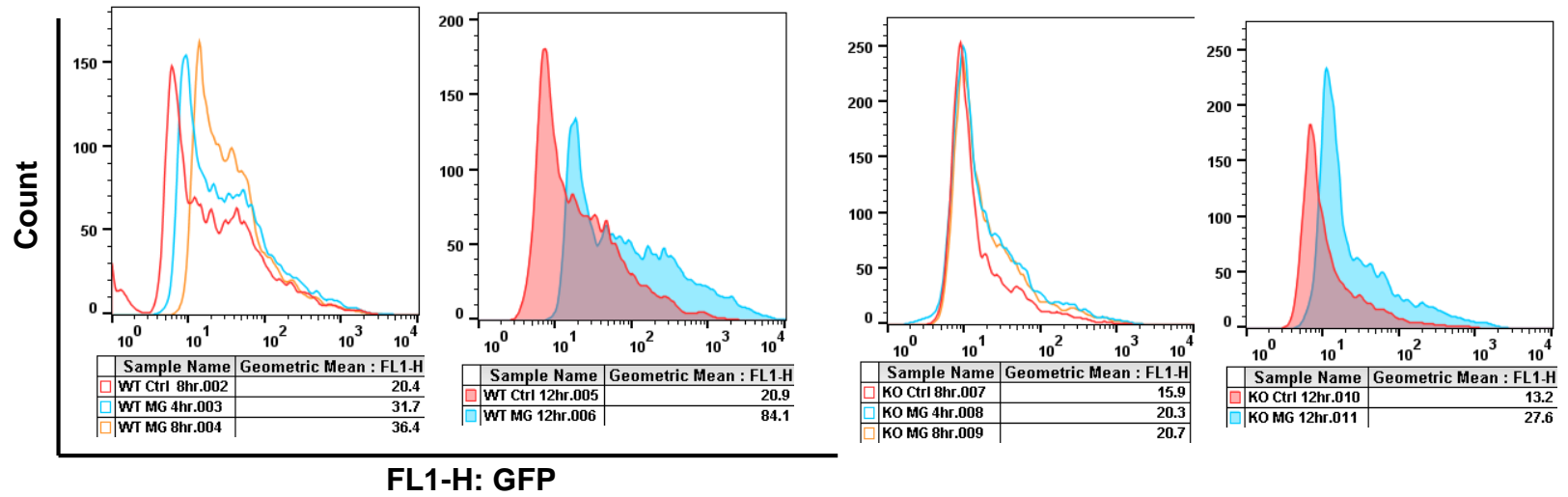
A**Whole cell****Nucleus****Cytoplasm****B**

Figure S5

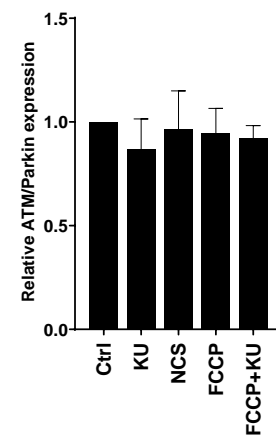
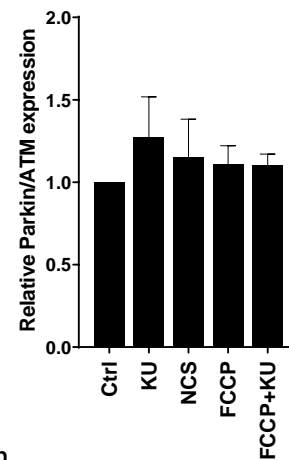
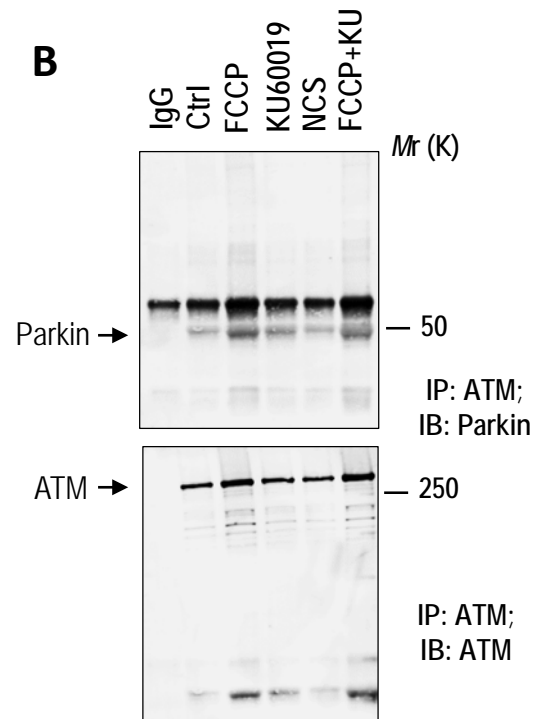
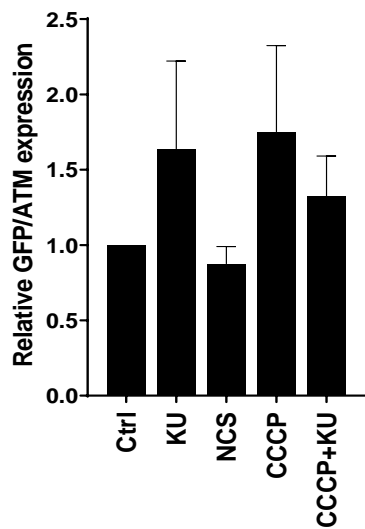
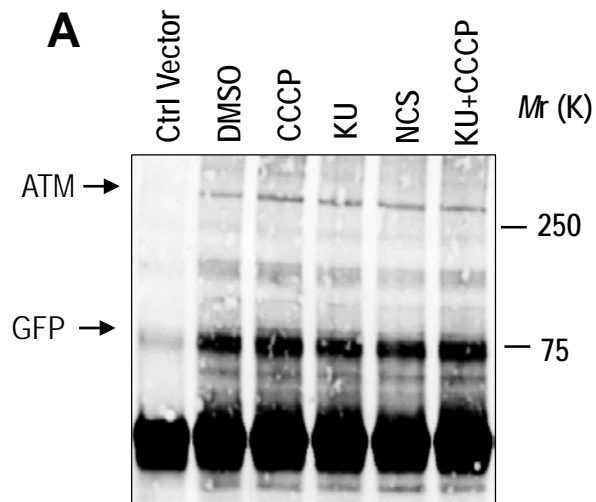


Figure S6

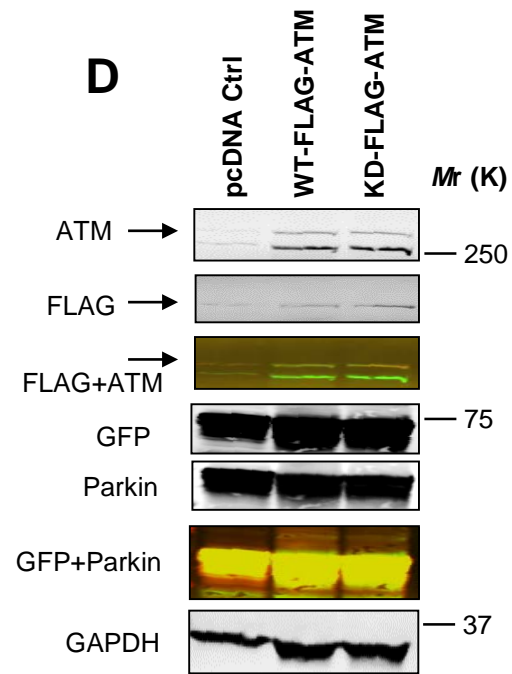
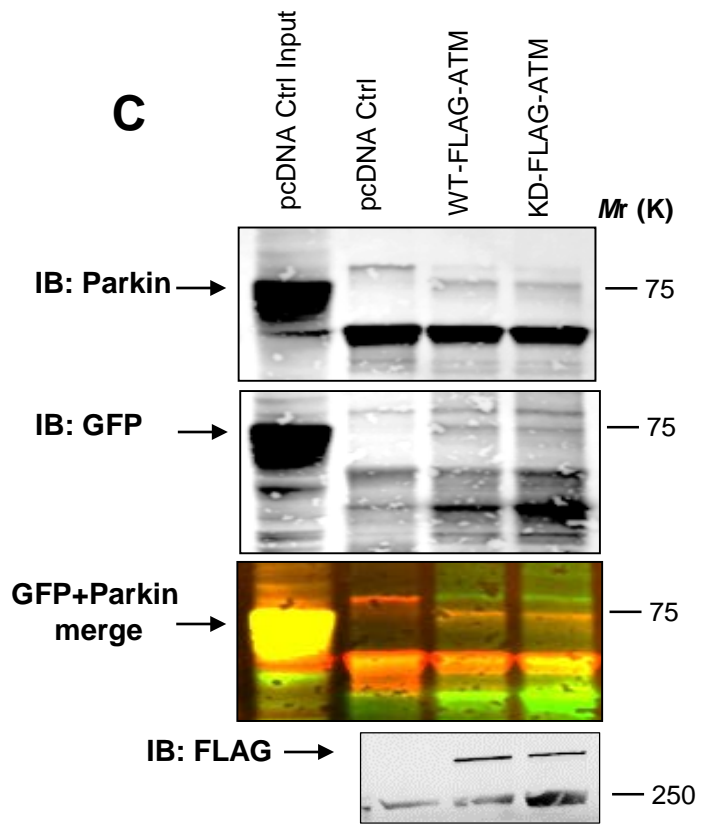


Figure S6 cont..

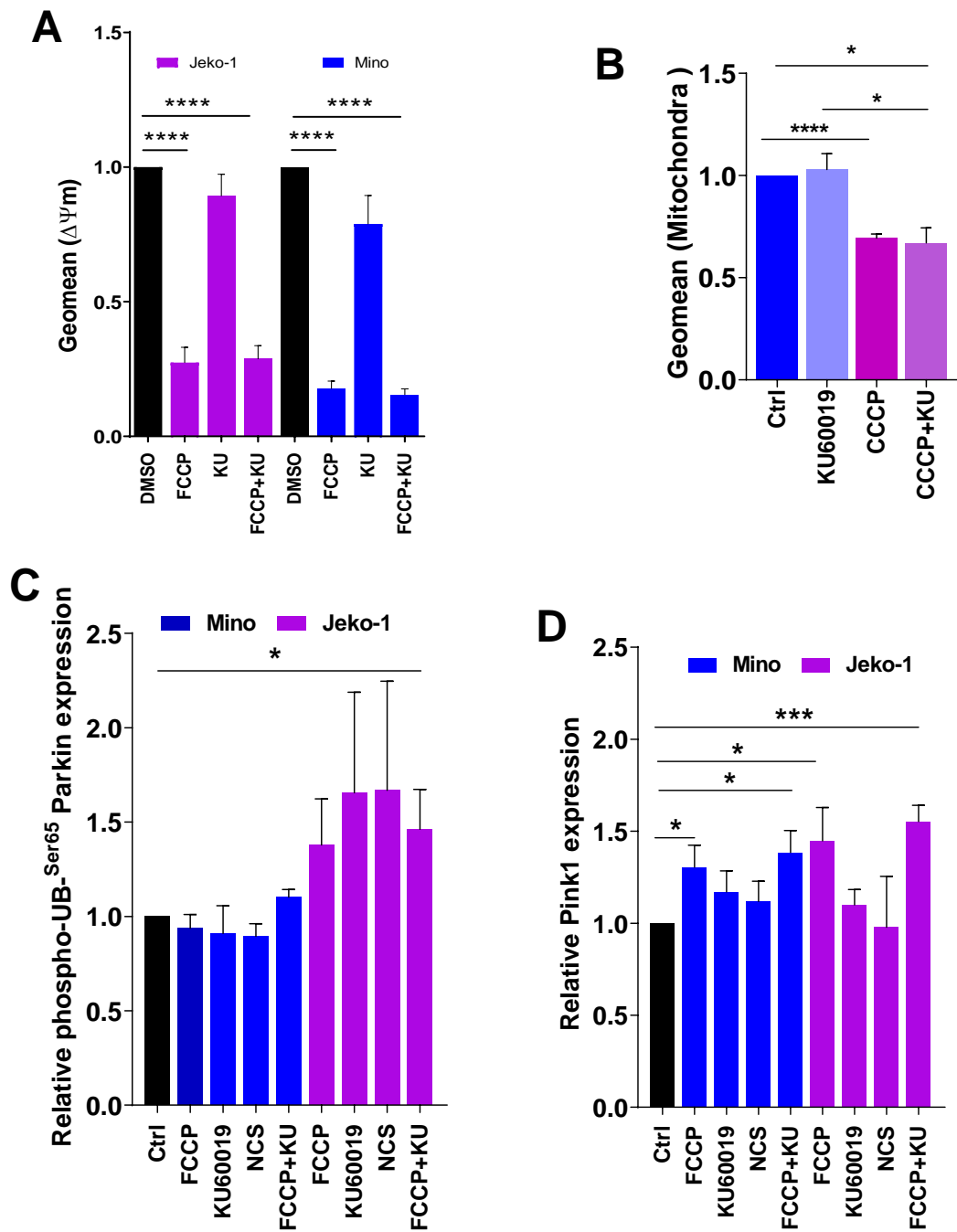


Figure S7

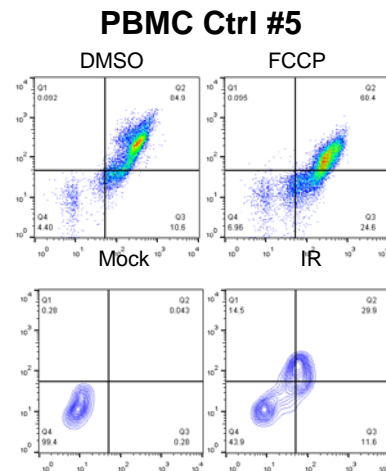
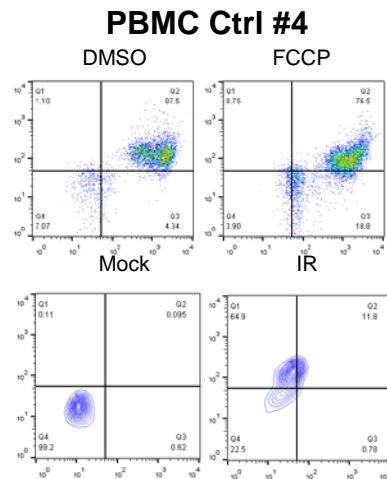
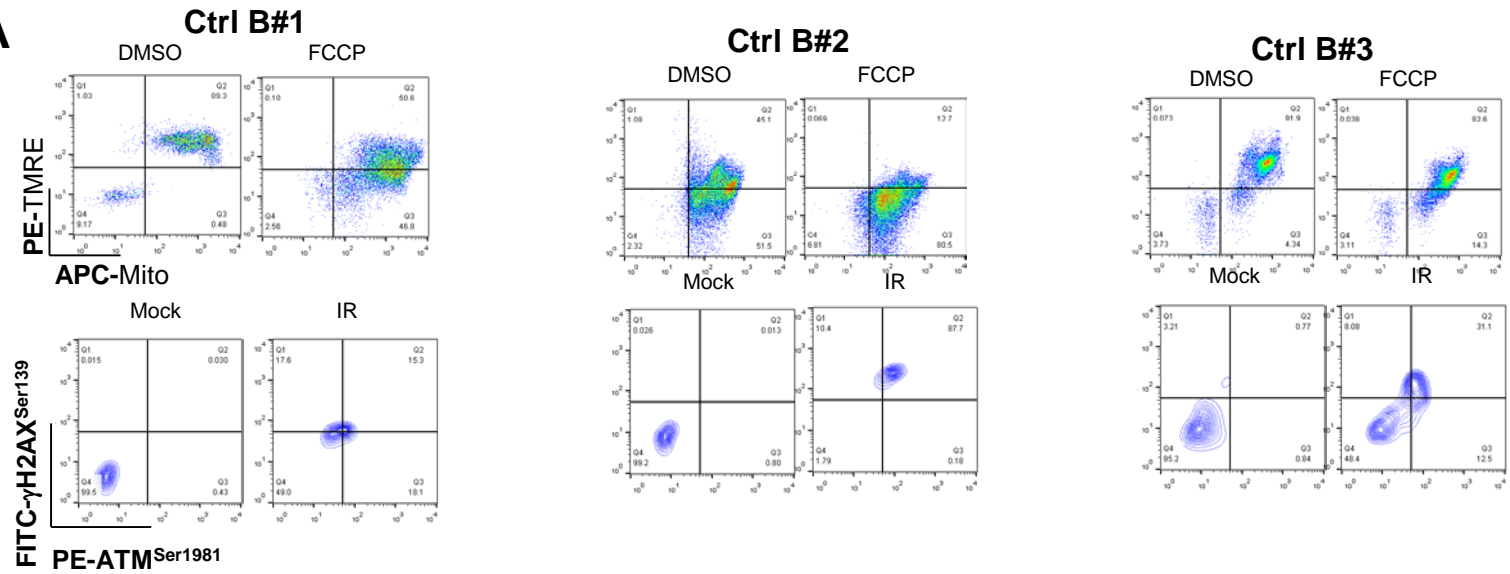
A

Figure S8

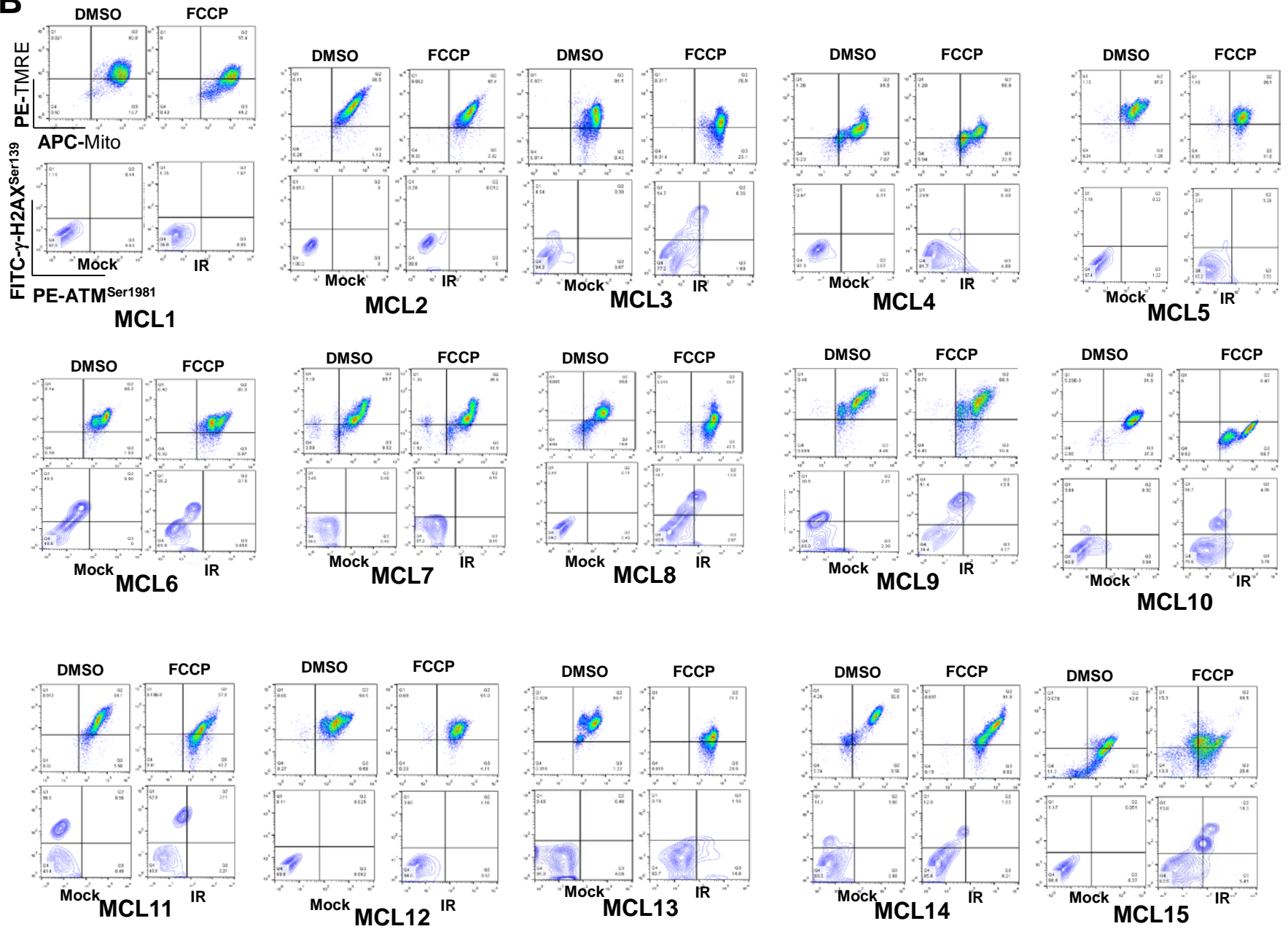
B

Figure S8 cont..

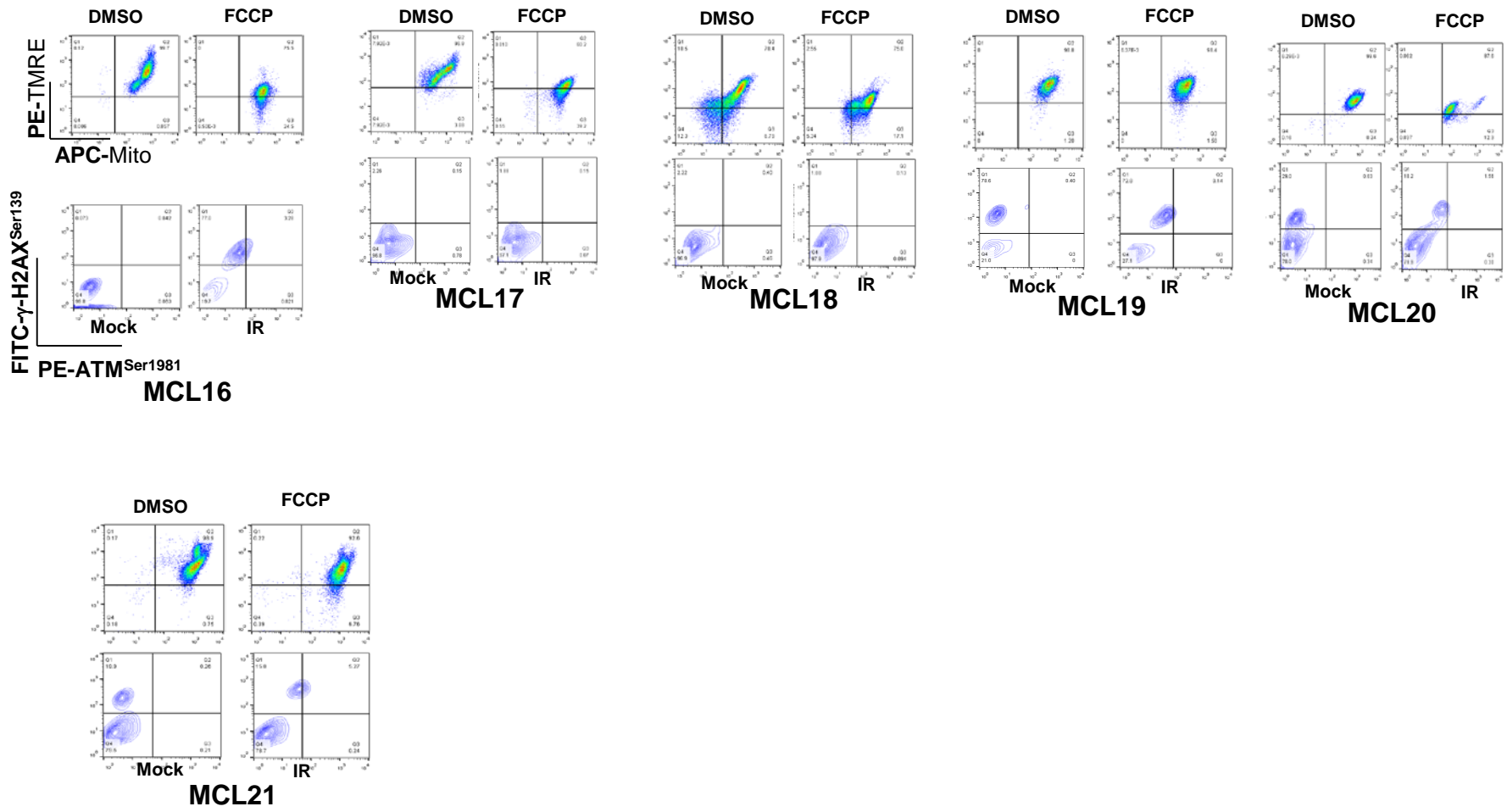


Figure S8 cont..

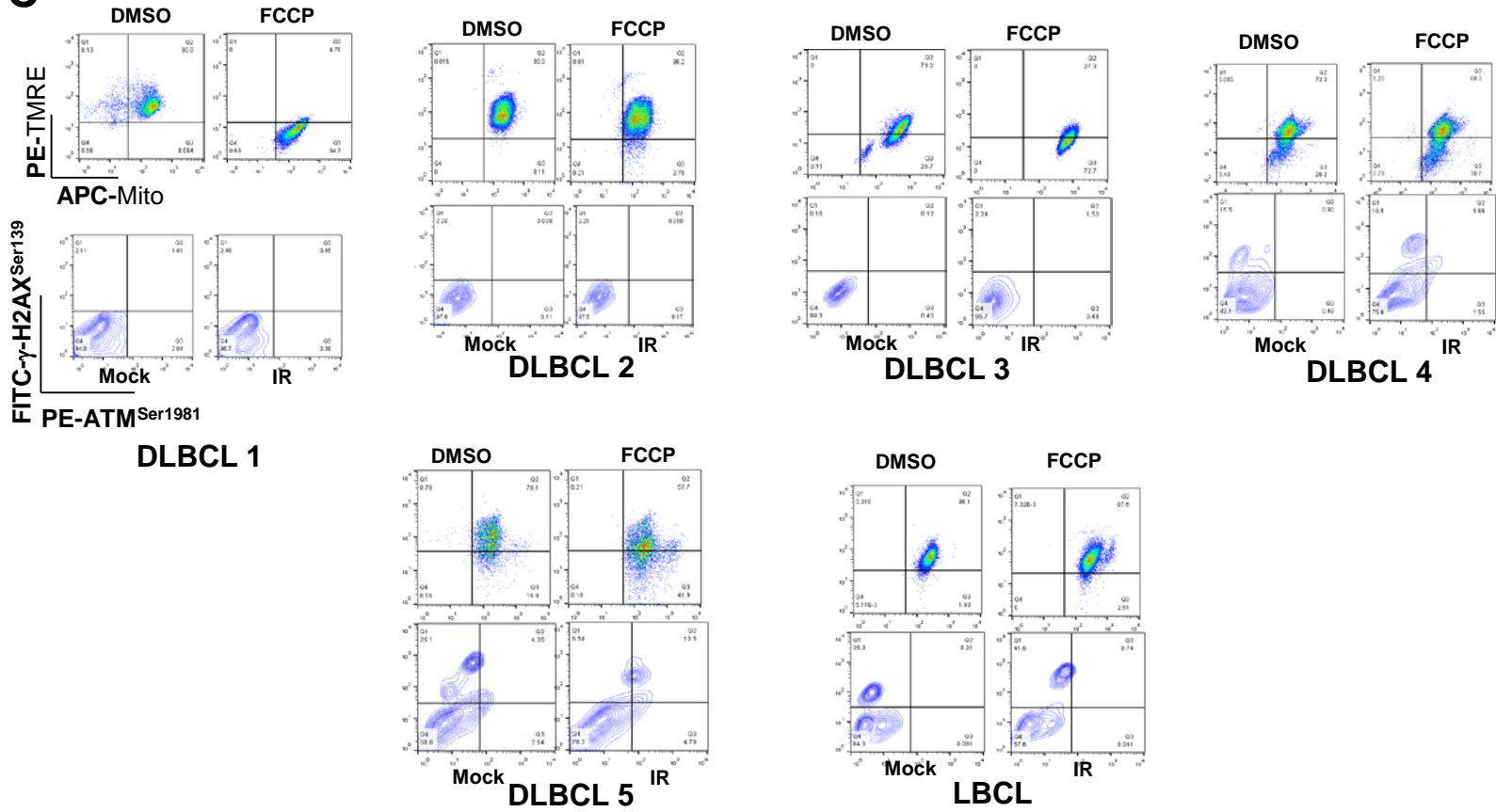
C

Figure S8 cont..

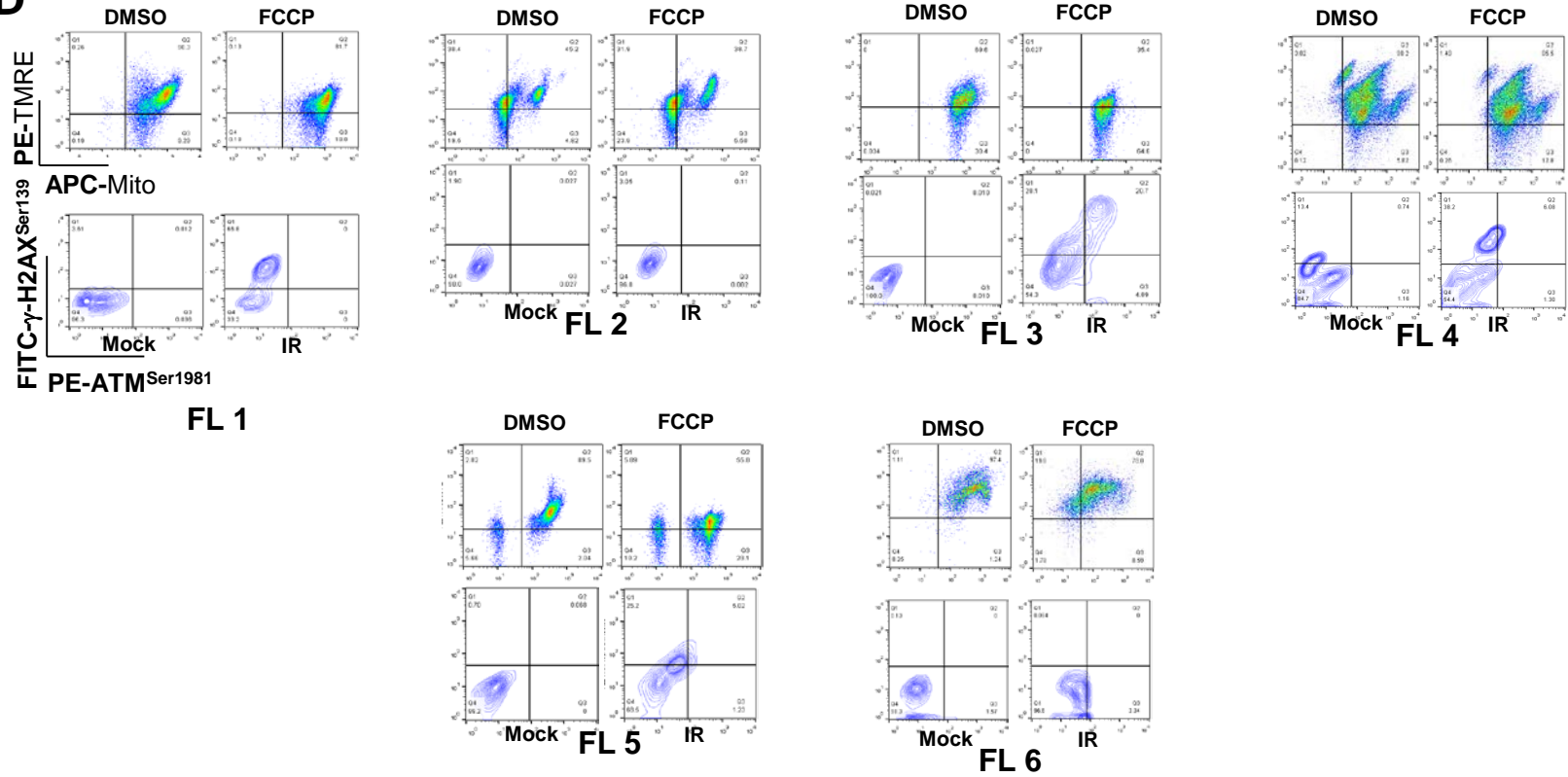
D

Figure S8 cont..

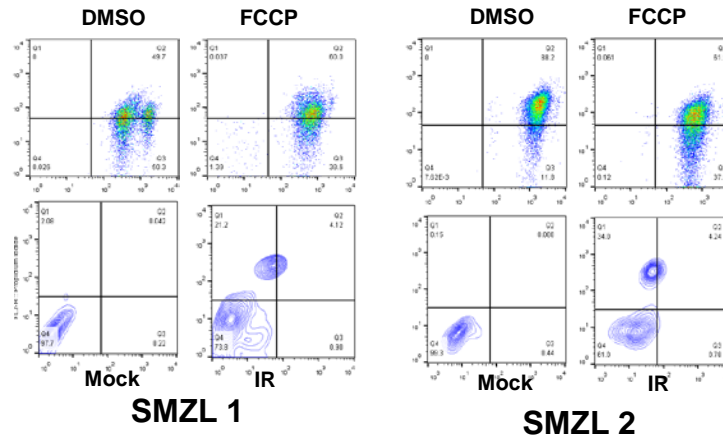
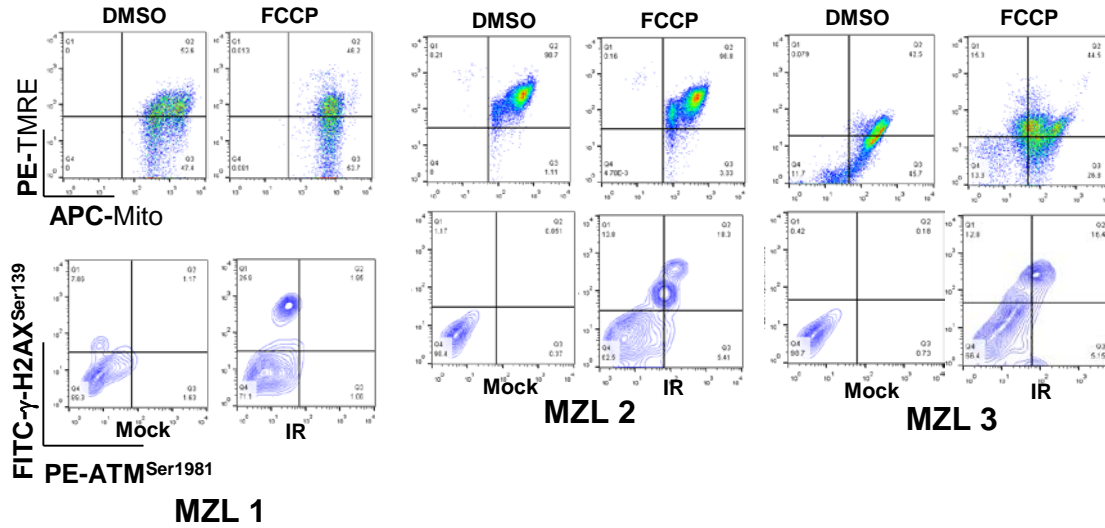
F

Figure S8 cont..

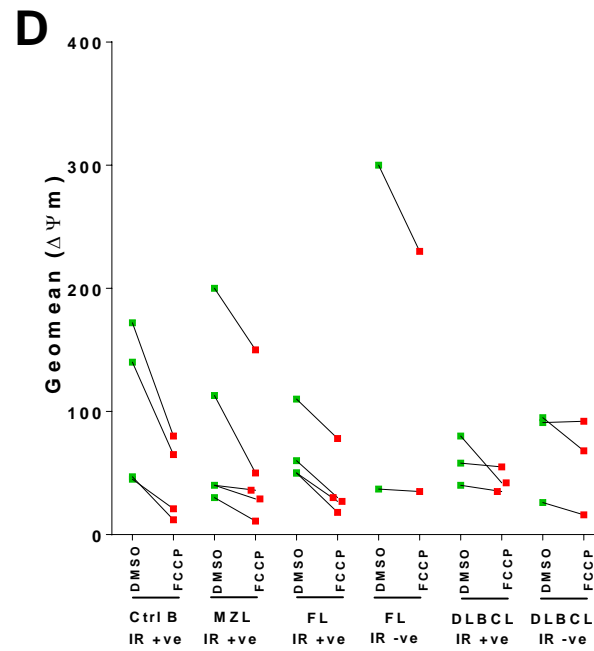
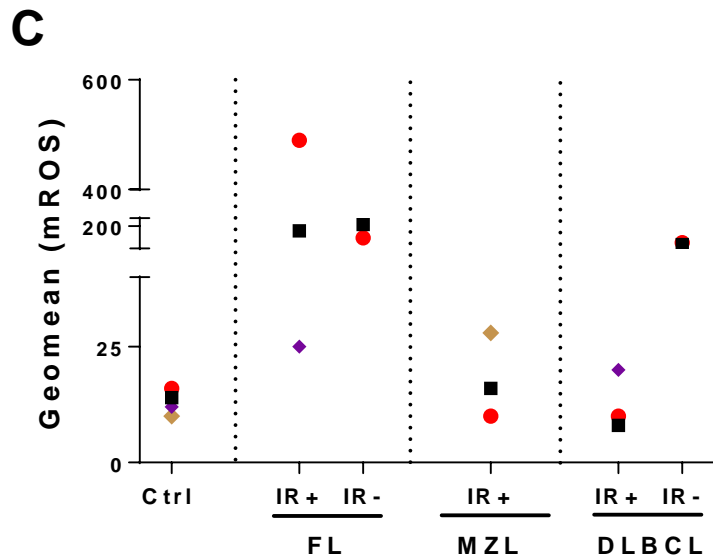
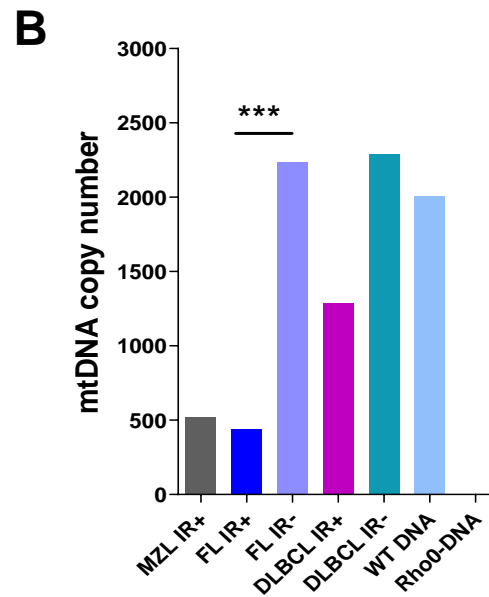
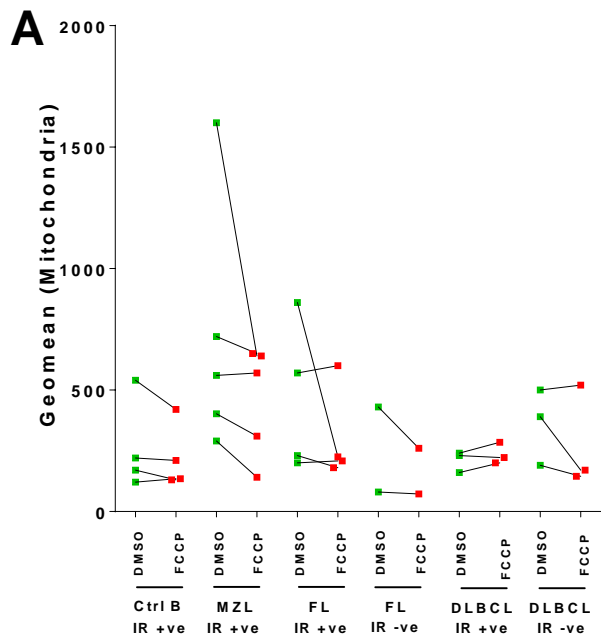
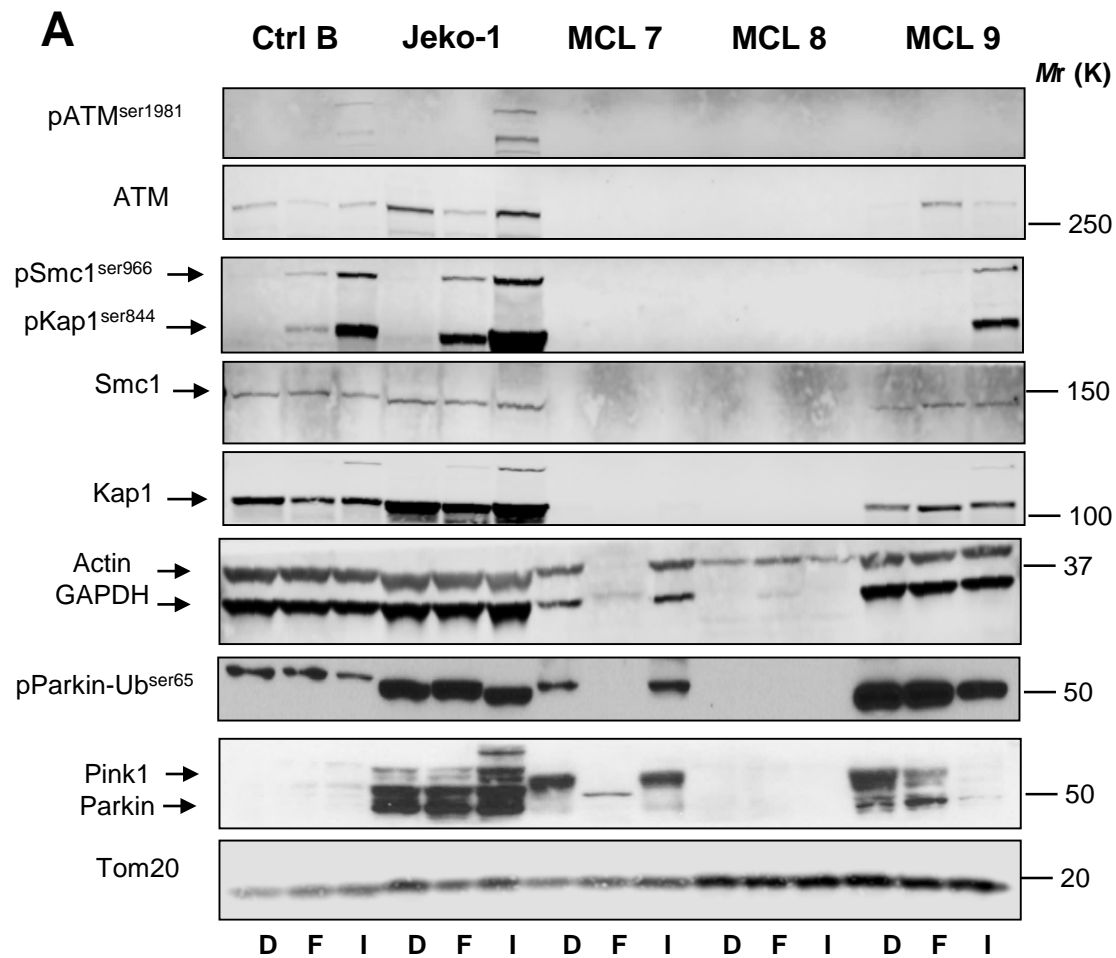


Figure S9



APC (Mito)	800	730		228	125		152	155		321	322		244	230	
$\Delta\Psi_m$	110	72		35	16		55	51		58	32		280	180	
IR			+			+			-			+			+
t11(14)	ND			ND			+			-			+		

D: DMSO
F: FCCP
I: IR

Figure S10

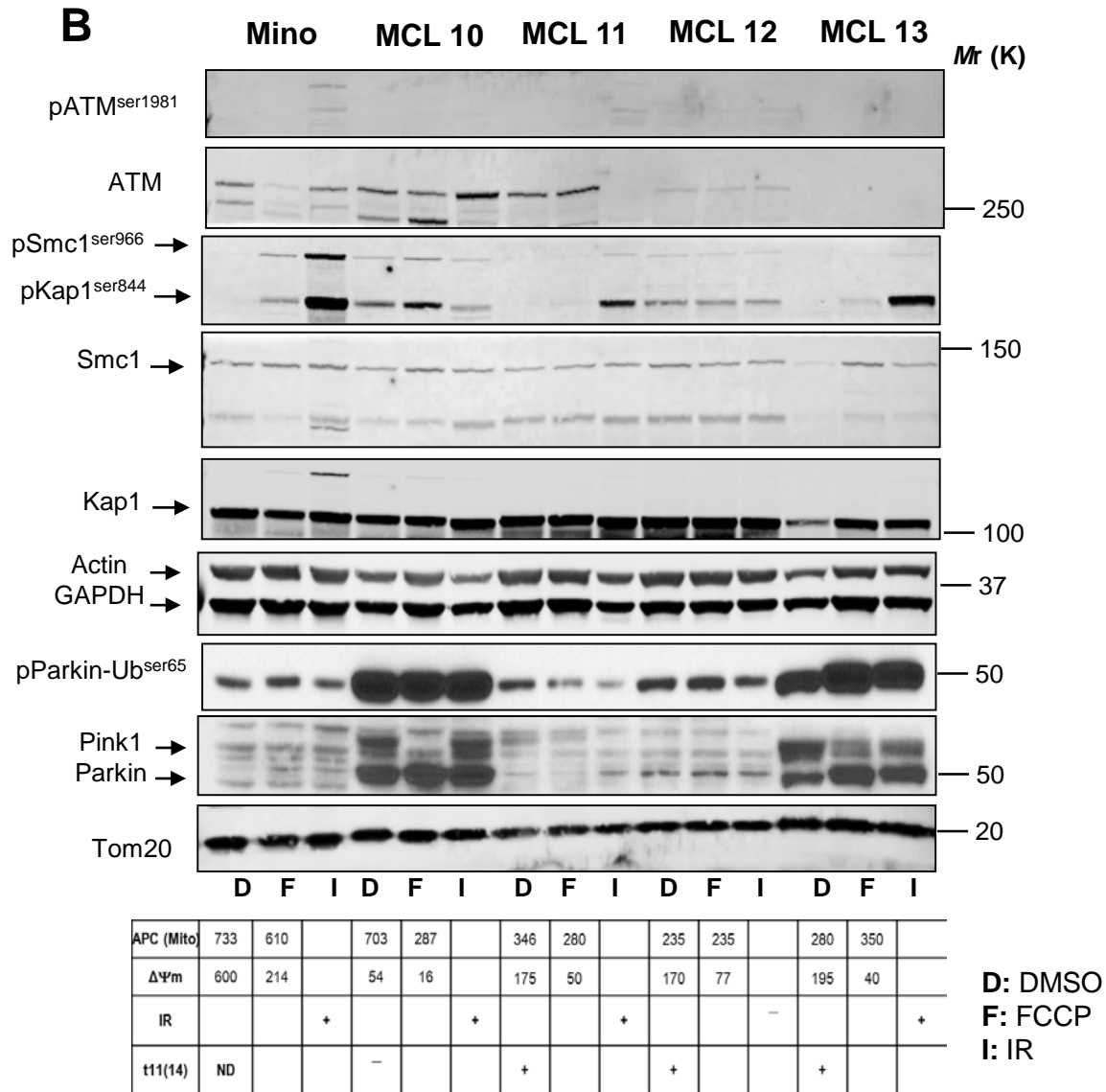


Figure S10 cont..

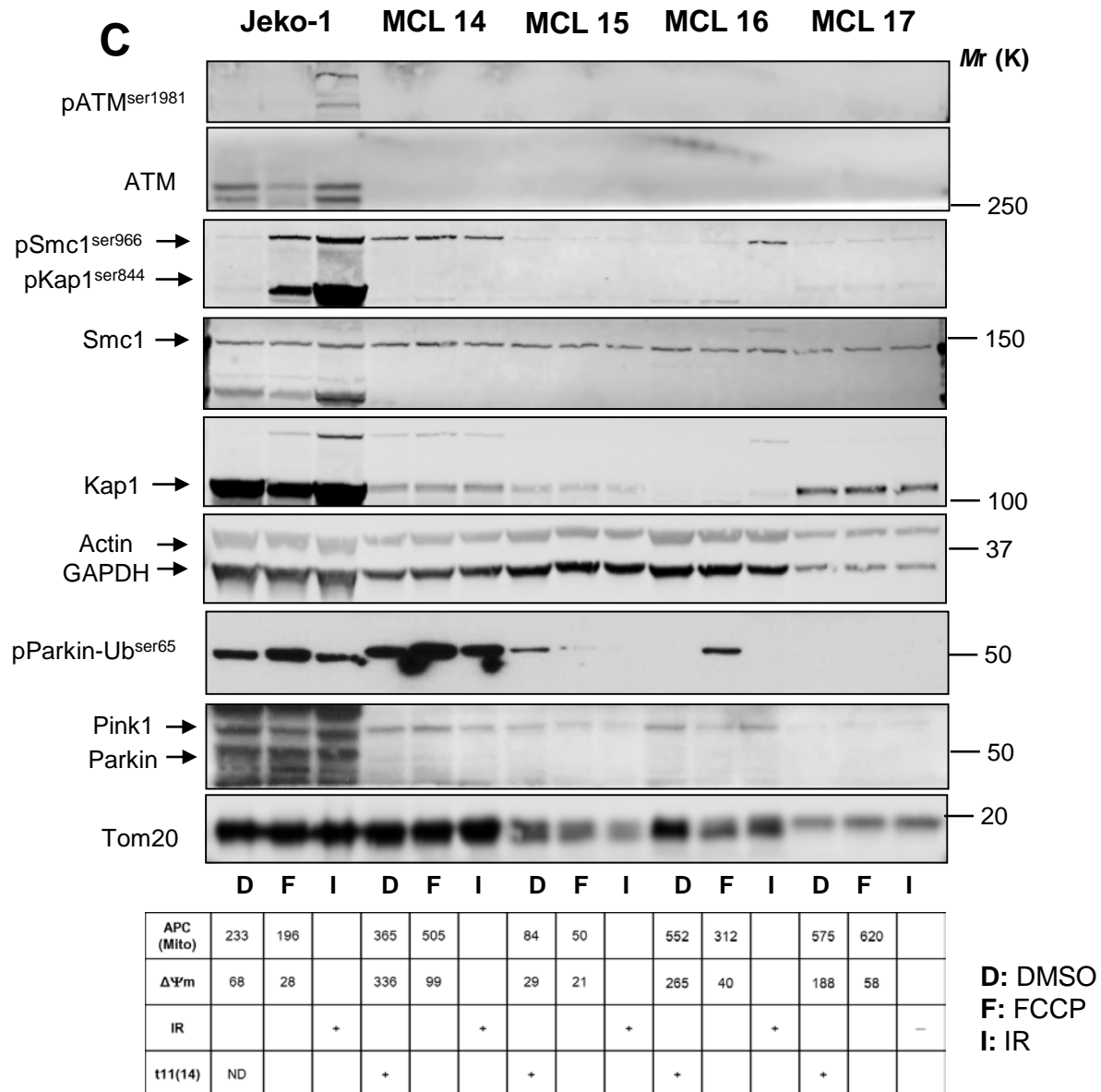
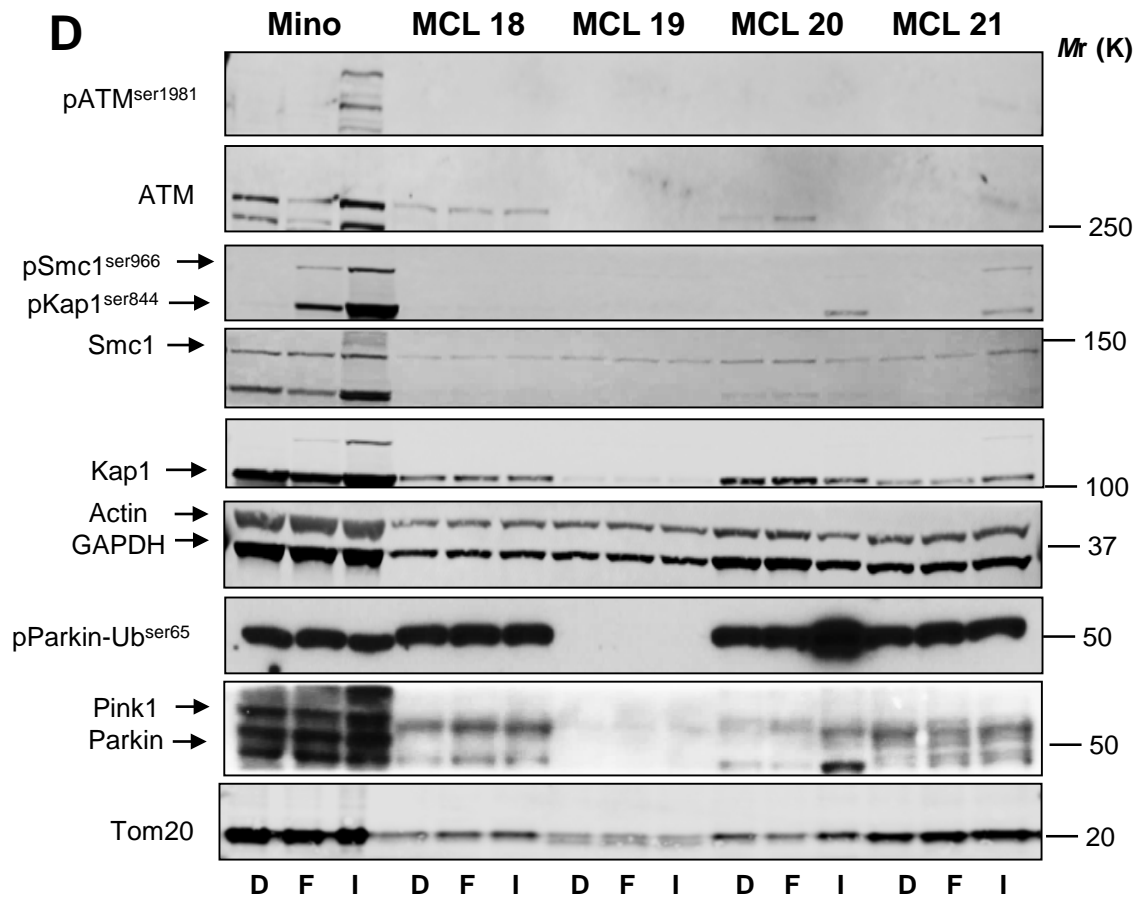


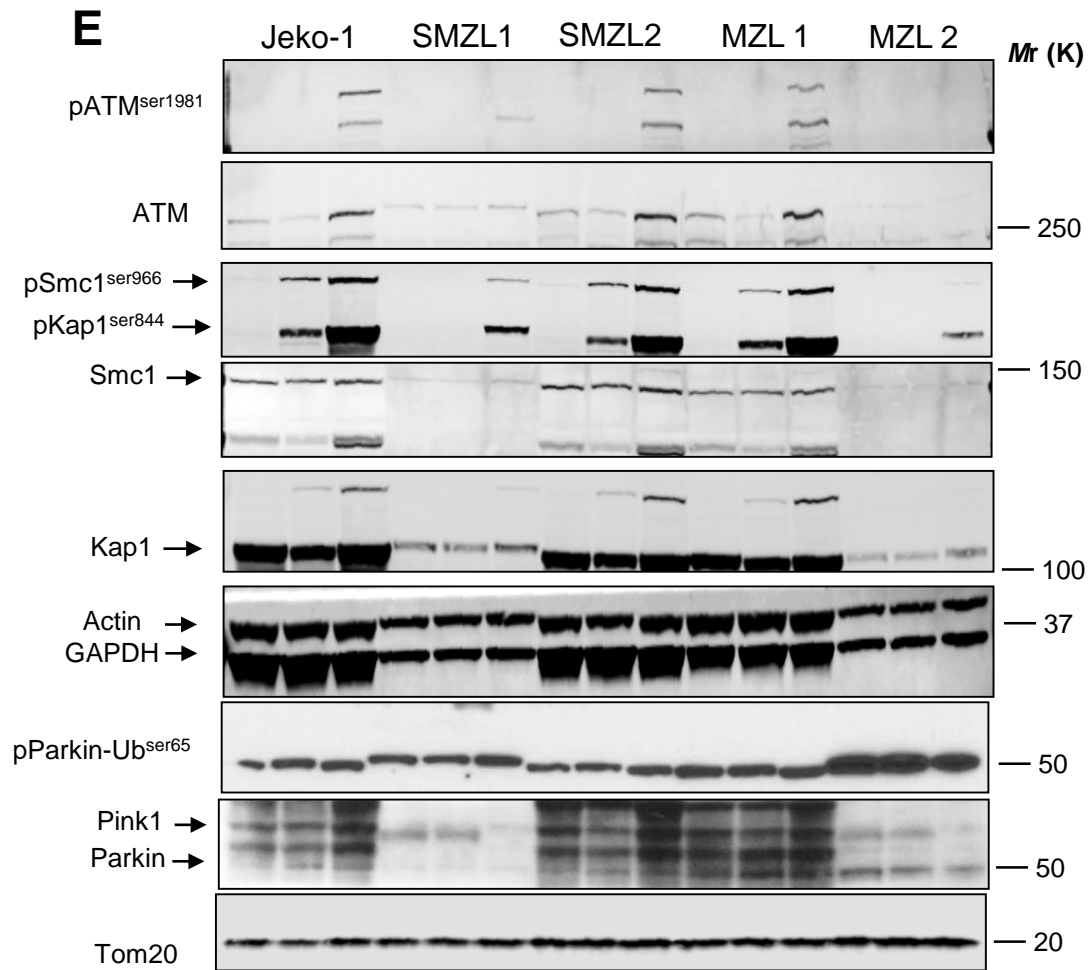
Figure S10 cont..



APC (Mito)	739	203		360	400		622	632		1120	660		1022	963	
$\Delta\Psi_m$	99	12		50	28		198	63		70	53		305	162	
IR			+			-			+			+			+
t11(14)	ND			+			+			+			+		

D: DMSO
F: FCCP
I: IR

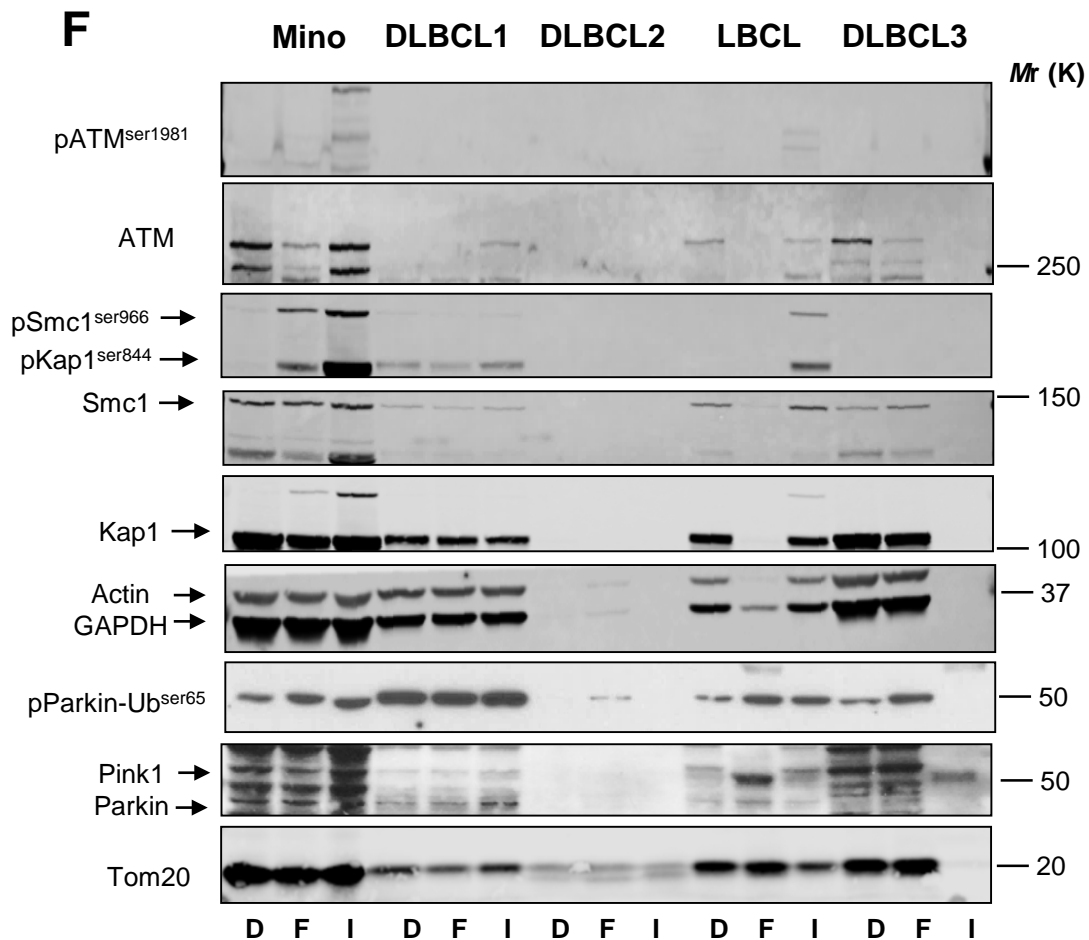
Figure S10 cont..



	Jeko-1			SMZL1			SMZL2			MZL 1			MZL 2		
	D	F	I	D	F	I	D	F	I	D	F	I	D	F	I
APC (Mito)	233	196		560	570		1600	640		720	650		402	310	
$\Delta\Psi_m$	68	28		40	36		113	50		40	29		200	150	
IR			+			+			+			+			+
t11(14)	ND			-			-			-			-		

D: DMSO
F: FCCP
I: IR

Figure S10 cont..

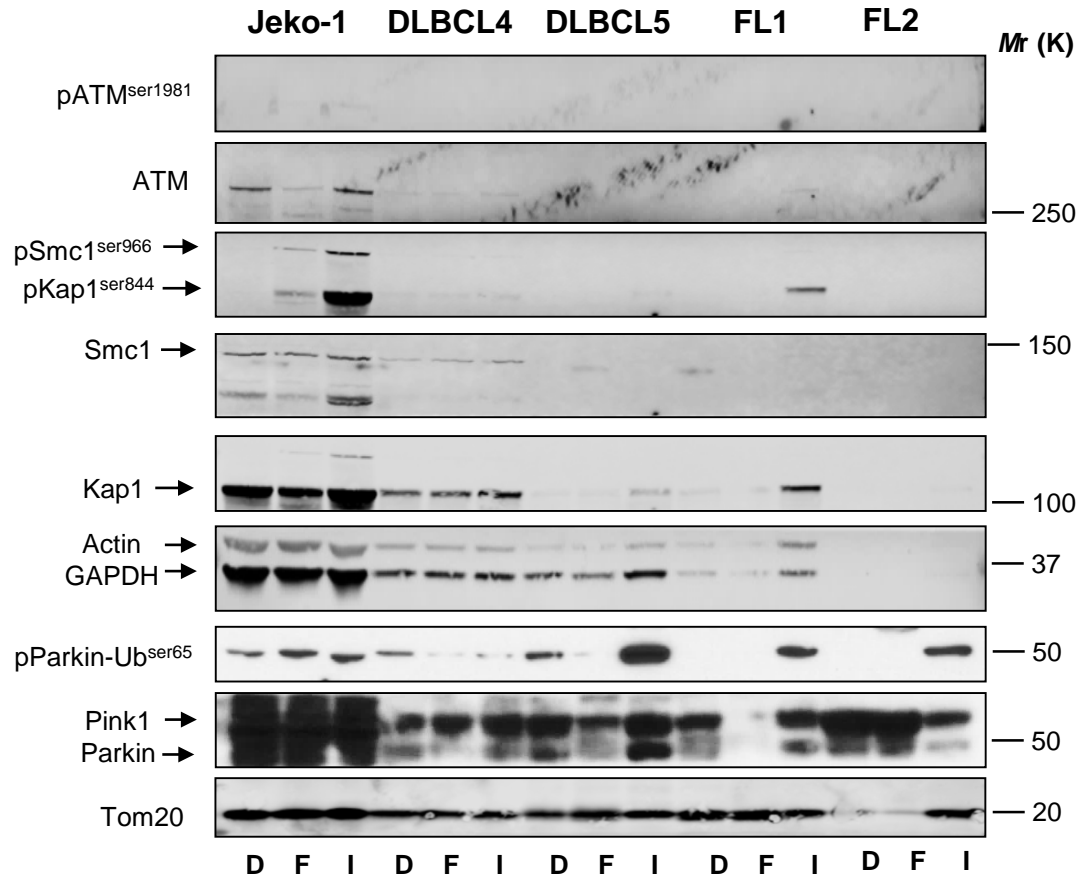


APC (Mito)	739	203		390	170		190	145		240	285		500	520	
$\Delta\Psi_m$	99	12		91	92		95	68		58	55		26	16	
IR			+			-			-			+			-
t11(14)	ND			ND			-			-			-		

D: DMSO
F: FCCP
I: IR

Figure S10 cont..

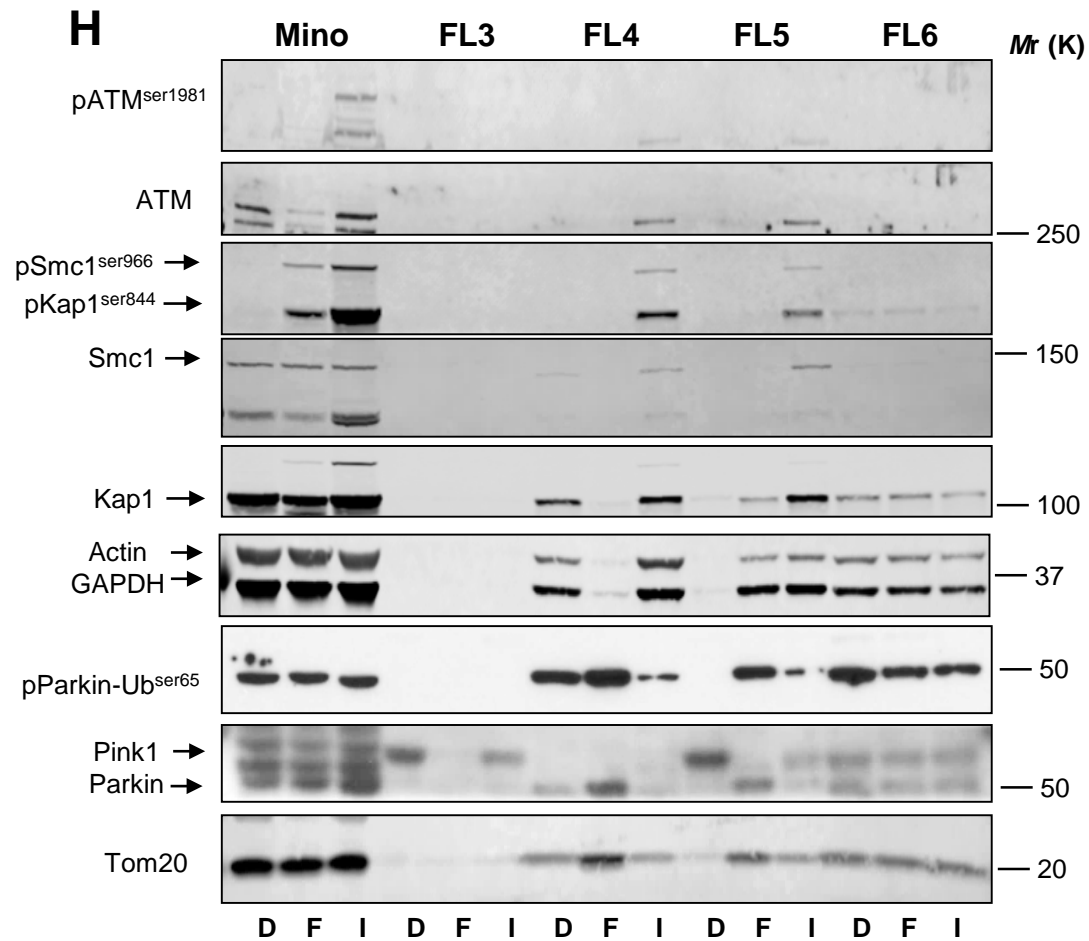
G



APC (Mito)	233	196		230	222		160	200		570	600		80	72	
$\Delta\Psi_m$	68	28		40	35		80	42		50	27		37	35	
IR			+			+			+			+			-
t11(14)	ND			-			-			-			-		

D: DMSO
F: FCCP
I: IR

Figure S10 cont..



APC (Mito)	739	203		860	225		200	208		230	180		430	260	
$\Delta\Psi_m$	99	12		60	30		110	78		50	18		300	230	
IR			+			+			+			+			-
t11(14)	ND			-			-			-			-		

D: DMSO
F: FCCP
I: IR

Figure S10

Supplementary Table 1: Antibodies used in the study.

Primary antibody	Ig type	Source	Catalogue number	Dilution
ATM	Rabbit	Millipore	07-1286	1000
ATM	Mouse	Santa Cruz	sc-23921	750
phospho-ATM ^{ser1981}	Mouse	Millipore	05-740	1000
p53	Mouse	Millipore	OP43	1000
phospho-p53 ^{ser15}	Rabbit	CST	9284	1000
Kap1	Mouse	GeneTex	GTX49179	1000
Kap1	Rabbit	Bethyl Lab	A300-274A	5000
phospho-Kap1 ^{ser824}	Rabbit	Bethyl Lab	A300-767A	2500
Smc1	Mouse	GeneTex	GTX82813	1000
pSmc1 ^{ser966}	Rabbit	GeneTex	GTX21276	1000
GAPDH	Mouse	GeneTex	GTX627408	7500
Actin	Mouse	Santa Cruz	sc-47778	1000
Actin	Rabbit	Proteintech	20536-1-AP	5000
LC3	Rabbit	SIGMA	L8918	1000
COXIV	Mouse	Life Technologies	A-21347	5000
Tom20	Rabbit	Santa Cruz	sc-11415	1000
Tom20	Mouse	Santa Cruz	sc-17764	1000
Lamin B1	Mouse	Proteintech	66095-1	5000
P62	Rabbit	Enzo	BML-PW9860-0100	5000
Parkin	Mouse	Santa Cruz	sc-32282	500
Parkin	Rabbit	MILLIPORE	AB-5112	1000
phospho-Parkin ^{ser65}	Rabbit	ABCAM	ab154995	1000
Pink1	Rabbit	CST	6946	1000
Pink1	Rabbit	Novus	BC-100-494	1000
GFP	Rabbit	GeneTex	GTX113617	2500
GFP	Rabbit	Santa Cruz	sc-8334	1000
FLAG	Mouse	SIGMA	F1804	2500
Anti DNA	Mouse	PROGEN	AC-30-10	10000
VDAC1	Rabbit	Proteintech	55259-1-AP	2000
TOM70	Rabbit	Santa Cruz	sc-366282	1000
TIM23	Mouse	Santa Cruz	sc-514463	750

Type	Sample type	Patient sex	Patient Age	Stage	Untreated/Relapsed	Supplemental Table S2: Patient characteristics						Tumor Cells %	Growth factor information	Cytogenetics	
						WBC	Lymp	Neut	Metam	Blasts	Monocytes				
1	MCL	Leukemic phase blood	Female	63	IV	Untreated	115	80.5	18.4	0	0	9.2	69%	No GF	48,XX,t(9;+4p+;+5p-;7q-;9p+;9q+;11;14),12p-,-13,-16,-17,-18,-18+19,-21,-22,+6mar[1]/46,XX[9]
2	MCL	Peripheral blood	Male	60	IV	Untreated	23.4	16.61	5.62	0	0	0.47	69%	No GF	t(11;14)
3	MCL	Leukemic phase blood	Male	63	IV	Untreated	46.7	39.26	4.67	0	0	0	90%	No GF	t(11;14),13q-,6q-
4	MCL	Leukemic phase blood	Male	66	IV	Relapsed	140.1	135.8	1.4	0	0	2.8	95%	No GF	46,XY,t(11;14)
5	MCL	Leukemic phase blood	Male	61	IV	Untreated	68.5	58.23	8.91	0	0	0	98%	No GF	46,XY,t(11;14)(q13;q32)
6	MCL	Fluid	Male	66	IV	Untreated	ND	ND	ND	ND	ND	ND	90%	No GF	46,XY
7	MCL	Leukemic phase	Female	49	IV	Untreated	19.1	14.68	3.62	0	0	0.57	75%	No GF	46,XX,del(9)(q12)[1] and t(11;14)
8	MCL	Apheresis	Female	46	IV	Untreated	46.2	42.01	1.38	0	0	0	94%	No GF	46,XY,t(11;14)(q13;q32)
9	MCL	Apheresis	Male	65	IV	Relapsed	103.5	87.94	12.42	0	0	3.1	85%	No GF	46,XY,inv(9)(p12q13),t(11;14)
10	MCL	Apheresis	Male	62	IV	Untreated	145.2	135.01	2.9	0	0	1.45	96%	No GF	46,XY,11q-and-11
11	MCL	Apheresis	Male	67	IV	Relapsed	102.2	85.66	8.18	0	0	1.02	95%	No GF	43,XY,-1,-5,add(6)(q13),add(7)(p22),del(10)(q24),t(11;14)(q13;q32),ins(12?)(q13?)-13,-20(1)46,XY[18]
12	MCL	Apheresis	Female	70	IV	Untreated	112.7	92.39	9.01	0	0	0	91%	No GF	45-47,XX,del(3)(q21),add(4)(q35),t(11;14)(q13;q32)-13,(17)(q10),+2-5mar[cp5]46,XX[15]; DELETION OF A SINGLE D13S319 LOCUS, DELETION OF A LAMP1 GENE AND A TP53 GENE DELETION.
13	MCL	Surgical Biopsy	Male	67	IV	Treated	ND	ND	ND	ND	ND	ND	ND	ND	44,XY,del(10)(p13),add(11)(p15),der(11)t(11;14)(q13;q32),add(14)(p11.2),der(14)t(11;14)add(11)(q22),add(19)(p13.3)+1-2mar[cp2]
14	MCL	Apheresis	Male	46	IV	Relapsed	105	17.85	19.95	0	0	0	96%	No GF	44-46,XY,der(2)inv(2)(p25q11.2)(2-12)(q31;q13),del(4)(q31.3q35),add(9)(p22),add(10)(q24),t(11;14)(q13;q32),der(12)t(2;12)(p11.2;p11.2)(2-12)(q31;q13),i(17)(q10)[cp8]
15	MCL	Leukemic phase blood	Female	63	IV	Relapsed	67.7	39.2	20.98	0	0	4.74	90%	No GF	46,XX,9p+;t(11;14)
16	MCL	Leukemic phase blood	Male	59	IV	Untreated	28.1	11.21	4.95	0	0	0	75%	No GF	46,XY,t(11;14)
17	MCL	Apheresis	female	77	IV	Untreated	74	60.66	4.44	0	0	0.74	86%	No GF	46,XX,t(8)(q10),t(11;14)(q13;q32),del(17)(p11.2),dup(17)(q21q25)[1] and 6,XX,der(2)t(2;14)(p23;q32)t(11;14)(q13;q32),t(8)(q10),der(11)t(11;14),der(14)t(14;14)(2-14),del(17)(p11.2),dup(17)(q21q25)[4]
18	MCL (blastoid)	Fluid	Male	72	IV	Untreated	ND	ND	ND	ND	ND	ND	90%	No GF	46,XY,t(11;14)
19	MCL	Leukemic phase	Male	61	IV	Untreated	71.4	60.69	5	0	0	0	94%	No GF	46,XY,t(11;14)(q13;q32)
20	MCL	Apheresis	Male	53	IV	Untreated	52	45.24	5.2	0	0	0.52	87%	No GF	46,XY,t(11;14)(q13;q32)
21	MCL	Leukemic phase blood	Male	69	IV	Relapsed	43.6	42.3	0.87	0	0	0.44	93%	No GF	44,XY,+1,der(1;9)(q10;q10),der(1;17)(q10;q10),add(4)(q35),t(11;14)(q13;q32),-13,add(15)(p11.2)[8]
22	SMZL (Marg Zone NHL, splenic)	Blood	Female	62	IV	Relapsed	4.6	1.73	2.46	0.01	0	0.28	ND	No GF	46,XX,t(12)(p35.1p33)[1] & Negative for t(11;14)
23	SMZL (Marg Zone NHL, splenic)	Peripheral blood	Male	78	IV	Untreated	63.4	55.16	6.34	0	0	1.27	ND	No GF	46,XY,del(7)(q22q34)
24	MZL (MZBL, NOS)	Leukemic phase blood	Male	42	IV	Untreated	82	78.72	2.46	0	0	0	90%	No GF	46,XY and DELETION OF BOTH D13S319 LOCI
25	MZL (Marg Zone NHL, splenic)	Leukemic phase blood	Female	74	IV	Untreated	34.1	28.29	4.77	0	0	0.68	83%	No GF	46,XX and TP53 gene deletion
26	MZL	Leukemic phase blood	M	35	IV	Relapsed	5.3	4.04	0.85	0	0	0.32	58%	No GF	46,XY
27	FL (Gr 1)	Fluid	Female	42	IV	Relapsed	ND	ND	ND	ND	ND	ND	86%	No GF	46,XX
28	FL (Gr 2/3) and DLBCL 20%	Surgical sample	Male	70	IV	Untreated	ND	ND	ND	ND	ND	ND	55%	No GF	46,XY
29	FL	Surgical biopsy	Male	50	III	Untreated	ND	ND	ND	ND	ND	ND	42%	No GF	46,XY,del(2)(q31q36),t(14;18)(q32;q21)
30	FL	Surgical biopsy	Male	70	IV	Untreated	ND	ND	ND	ND	ND	ND	66%	No GF	46,XY
31	DLBCL	Leukemic phase blood	Male	72	IV	Untreated	41.1	34.93	4.93	0	0	0.41	81%	No GF	46,XY,del(1)(p32p36.1)
32	DLBCL	Pleural fluid	Male	45	IV	Relapsed	ND	ND	ND	ND	ND	ND	96%	No GF	48-50,X,-Y,del(1)(p32p36.1)+3,add(3)(p25),add(3)(p13)+5,add(6)(q22),del(6)(q13q24)+7,add(8)(q23),add(9)(p12),del(9)(p13),add(11)(p15),add(12)(q24.3),ins(13;7)(q13;7),del(17)(p11.2),add(19)(q13.3)+2-4mar[cp12]
33	DLBCL	Fluid	Male	48	IV	Relapsed	ND	ND	ND	ND	ND	ND	90%	No GF	46,XY
34	FL (Gr 2)	Fluid	Male	55	IV	Untreated	ND	ND	ND	ND	ND	ND	ND	No GF	ND
35	FL	Fluid	Male	77	IV	Relapsed	ND	ND	ND	ND	ND	ND	ND	No GF	ND
36	DLBCL	Fluid	Male	70	IV	Relapsed	2.6	0.05	2.26	0	0	0.23	75%	No GF	ND
37	DLBCL	Leukemic phase blood	Male	73	IV	Relapsed	66.4	64.4	1.33	0	0	0.66	94%	No GF	47,XY,add(1)(p36.3),del(2)(q31q37),del(6)(q13q25),del(9)(q1q31),del(13)(q12q22),add(17)(p11.2),+18[15]
38	DLBCL	Fluid	Female	72	IV	Relapsed	ND	ND	ND	ND	ND	ND	90%	No GF	ND

ND: Not determined

Supplementary Table S3: Response of Non-MCL lymphomas in FCCP induced Mitophagy

	Lymphoma type	IR status	Mitophagy		$\Delta\Psi_m$ Status		mROS	mtDNA copy number
			DMSO	FCCP	DMSO	FCCP		
22	DLBCL 1	–	390	170	91	92	72	1412
23	DLBCL 2	–	190	145	95	68	85	2610
24	DLBCL 3	–	500	520	26	16	96	2856
25	DLBCL 4	+	230	222	40	35	10	1592
26	DLBCL 5	+	160	200	80	42	20	1611
27	LBCL	+	240	285	58	55	8	671
28	FL 1	+	570	600	50	27	25	296
29	FL 2	–	80	72	37	35	211	2304
30	FL 3	+	860	225	60	30	170	404
31	FL 4	+	200	208	110	78	ND	296
32	FL 5	+	230	180	50	18	490	774
33	FL 6	–	430	260	300	230	126	2165
34	MZL 1	+	720	650	40	29	10	845
35	MZL 2	+	402	310	200	150	ND	503
36	MZL 3	+	290	141	30	11	28	396
37	SMZL 1	+	560	570	40	36	16	435
38	SMZL 2	+	1600	640	113	50	10	414

ND: Not determined